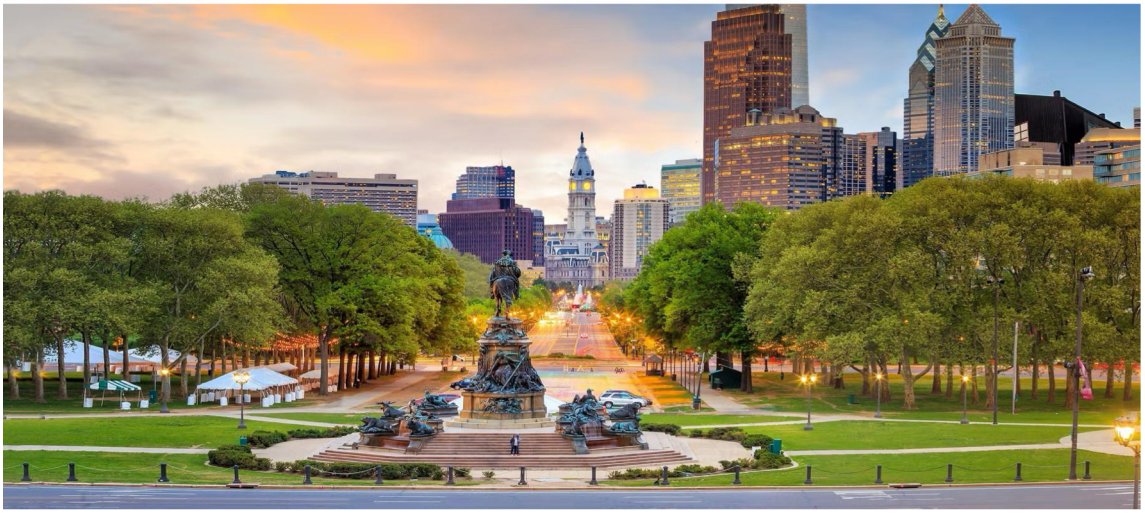
54th Annual Philadelphia Workshop on Hemostasis, Thrombosis and Atherosclerosis 2026



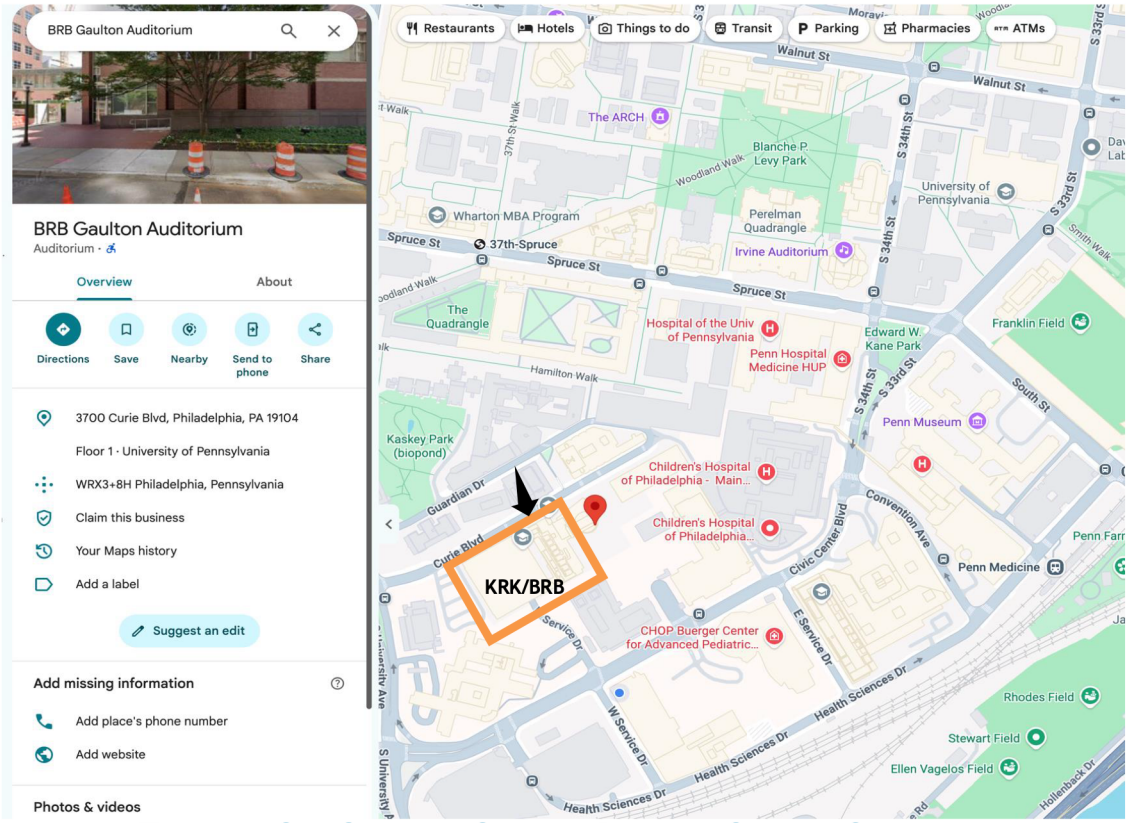
Thursday, November 5, 2026

At The Glen N. Gaulto Auditorium

William and Lois Kelley Research Building (KRB) formerly known as Biomedical Research Building (BRB)

421 Curie Boulevard, Philadelphia, PA 19104

Map for The Glen N. Gaulton Auditorium at the William and Lois Kelley Research Building (KRB/BRB)



Participating Institutions

Children's Hospital of Philadelphia

Penn — University of Pennsylvania

Temple University

Jefferson — Thomas Jefferson University — Home of Sidney Kimmel Medical College

Virginia Tech

Rutgers — The State University of New Jersey

Drexel University

The Rockefeller University — 1901 — Scientia Pro Bono Humani Generis

The Children's Hospital of Philadelphia *presents*

The 54th Annual Philadelphia Workshop on Hemostasis, Thrombosis, & Atherosclerosis

A full day of scientific exchange in hematology – insights into basic, clinical, and translational research in coagulation, platelet biology, and blood therapies

DATE	TIME	LOCATION
NOVEMBER 5, 2026	9 AM – 6 PM	At William and Lois Kelley Research Building (KRB) Gaulton Auditorium, University of Pennsylvania, 3700 Curie Blvd, Philadelphia, PA 19104

KEYNOTE SPEAKER



Jorge A. Di Paola, MD

EVP and Chief Scientific Officer

Associate Dean of Research and Professor of Pediatrics at Medical College of Wisconsin

KEYNOTE LECTURE

"Chronic inflammation reprograms the bone marrow to generate hyperactive platelets"

PROGRAM AT A GLANCE

9:00-9:30 AM	Breakfast and Coffee
9:30-12:30 AM	Abstract Presentations
12:30-2:00 PM	Lunch & Vendor Show KRB lobby
1:00-2:00 PM	Poster Presentations KRB lobby
2:10-3:10 PM	Keynote Lecture
2:10-3:10 PM	Abstract Presentations
4:50-6:00 PM	Reception and Awards KRB lobby

Special Thanks

We are very grateful to many of our colleagues who helped make this meeting a success. Thank you very much for your efforts.

Abstract Reviewers:

Lubica Rauova, MD, PhD - Children's Hospital of Philadelphia
Shekhar Kumar, PhD - Children's Hospital of Philadelphia
Osheiza Abdulmalik, DVM - Children's Hospital of Philadelphia
Wenchao Song, PhD - University of Pennsylvania
James Michael, PhD - Thomas Jefferson University
Amit Srivastava, PhD - Thomas Jefferson University
Lauren Poole, PhD - Rutgers University
Julie Goswami, MD - Rutgers University

Oral and Poster Judges:

Sriram Krishnaswamy, PhD - Children's Hospital of Philadelphia
Lawrence (Skip) Brass, MD, PhD - University of Pennsylvania
Koneti Rao, MD - Lewis Katz School of Medicine at Temple University
Shekhar Kumar, PhD - Children's Hospital of Philadelphia
Christopher S. Thom, MD, PhD - Children's Hospital of Philadelphia
Michele Lambert, MD - Children's Hospital of Philadelphia
Lubica Rauova, MD, PhD - Children's Hospital of Philadelphia
Peisong Ma, PhD - Thomas Jefferson University
Larry Goldfinger, PhD - Thomas Jefferson University
Valerie Tutwiler, PhD - Rutgers University
David Essex, MD - Lewis Katz School of Medicine at Temple University
Rodney Camire, PhD - Children's Hospital of Philadelphia
Matthew Bunce, PhD - Children's Hospital of Philadelphia
Nabil Thalji, MD, PhD - University of Pennsylvania
Ekaterina Grishchuk, PhD - University of Pennsylvania

Oral Session Chairs:

Shekhar Kumar, PhD - Children's Hospital of Philadelphia
Amrita Sarkar, PhD - Children's Hospital of Philadelphia
Francis Ayombil, PhD - Children's Hospital of Philadelphia
James Michael, PhD - Thomas Jefferson University
Timothy Stalker, PhD - Thomas Jefferson University
Valerie Tutwiler, PhD - Rutgers University
Lauren Poole, PhD - Rutgers University

Organizing Committee:

Mortimer Poncz, MD - Children's Hospital of Philadelphia
Sriram Krishnaswamy, PhD - Children's Hospital of Philadelphia
Amrita Sarkar, PhD - Children's Hospital of Philadelphia
Francis Ayombil, PhD - Children's Hospital of Philadelphia
Timothy Stalker, PhD - Thomas Jefferson University
James Michael, PhD - Thomas Jefferson University
Valerie Tutwiler, PhD - Rutgers University
Lauren Poole, PhD - Rutgers University

We gratefully acknowledge **Vernell Wynn (CHOP), Terese Manganaro (UPenn), and Rachel Juster (CHOP)** for their outstanding efforts and dedication in planning and coordinating numerous aspects of the meeting.

Schedule of Events 2026:

9:00-9:30 **Welcome: Registration and Breakfast (KRB lobby)**

9:30-9:35 **Introductory remarks** by **Lawrence (Skip) Brass, MD, PhD**, Chief, Non-Malignant Hematology, University of Pennsylvania School of Medicine Director, Blood Center at PENN/CHOP Vice Chair for Research & Chief Scientific Officer, University of Pennsylvania School of Medicine (KRB Auditorium)

9:35-10:50 **Session #1 Platelet Biology & Thrombus Formation (KRK Auditorium)**

Chairs: Amrita Sarkar, PhD (CHOP) and James Michael (Jefferson)

9:35-9:50 *Abstract #23:* ***Amir Yarahmadi*** *(TJU) Modulation of BAK1 Expression by Megakaryocyte/Platelet-Targeted siRNA Reduces Apoptotic Changes and Promotes Platelet Survival*

9:50-10:05 *Abstract 25#:* ***Catherine House*** *(UPENN) Platelet Microarchitecture Regulates Coagulation Factor Transport and Reaction Rates in Three-Dimensional Reconstructions of Hemostatic Thrombi*

10:05-10:20 *Abstract #4:* ***Hannah Thomson*** *(TJU) A common GRK5 variant enhances PAR1-dependent platelet procoagulant activity and thrombin generation*

10:20-10:35 *Abstract #35:* ***Sophia Lazar*** *(TJU) Inflammatory Pathways Regulate Cytokine Responses and Thrombotic Burden in Heparin-Induced Thrombocytopenia*

10:35-10:50 *Abstract #26:* ***Harriet Ghansah*** *(TJU) Platelet-selective naked modified siRNA suppression of prostacyclin pathway mediators improves hemostasis in mice*

10:50-11:10 **Coffee Break**

KRB Lobby

11:10-12:25 **Session #2 Immune Thrombosis, Platelets & Vascular Biology**

Chairs: Shekhar Kumar, PhD (CHOP)) and Timothy J. Stalker, PhD (Jefferson)

11:10-11:25 *Abstract #11:* ***Gina Capece*** *(Rutgers) PAD4 deficiency increases APAP-induced liver injury independent of NET formation*

11:25-11:40 *Abstract #7:* ***Jenna Oberg*** *(CHOP) PF4-Centric Immunothrombotic Disorders Depend on Terminal Complement Activation and Are Responsive to C5 Inhibition*

11:40-11:55 *Abstract #34:* ***Olivia Parker*** *(Rutgers) Hemostatic and Inflammatory Changes After SCI: Determining Temporal Coagulation and Neutrophil Dynamics*

11:55-12:10 *Abstract #3:* ***Isabelle Chen*** *and* ***Diana Hnin*** *(CHOP) Maternal and fetal complications in Obstetric Antiphospholipid Syndrome (OAPS) are Platelet Factor 4 (PF4)-dependent*

12:10-12:25 *Abstract #24:* ***Jared Whitman*** *(TJU) Platelet FcγRIIA drives thrombo-inflammatory reperfusion injury following ischemic stroke through PLCγ2-dependent and PLCγ2-independent mechanisms*

12:30-2:00	**Lunch and Vendor Show**

KRB Lobby

1:00-2:00	**Poster Session (Authors present 1:15-2:00)**

KRB Lobby

2:10-3:10	**Keynote Lecture (KRB Auditorium)**

Introduction by: Morty Poncz, Professor of Pediatric, Jane Fishman Grinberg Endowed Chair in Stem Cell, Division of Hematology at Children's Hospital of Philadelphia, University of Pennsylvania.

Jorge DiPaola, MD

Professor of Pediatrics, Hematology & Oncology
Elizabeth Finney McDonnell Chair in Pediatric Hematology/Oncology Division Chief, Division of Hematology & Oncology

Title of lecture*:*

"Chronic inflammation reprograms the bone marrow to generate hyperactive platelets"

3:10-3:30	**Coffee Break**

KRB Lobby

3:30-4:45	**Session #3: Coagulation Factor Engineering, Structure & Therapeutic Innovation (KRK Auditorium)**

Chairs: Francis Ayombil, PhD (CHOP) and Lauren Poole, PhD (Rutgers)

3:30-3:45 *Abstract #32:* ***Shekhar Kumar*** *(CHOP) Engineering a Multifunctional Factor V to Effectively Support Both Intrinsic Tenase and Prothrombinase Functions*

3:45-4:00 *Abstract #33:* ***Jon Lindgren*** *(CHOP) A liver sinusoidal endothelial cell (LSEC)-directed genome editing platform for targeted integration at the F8 locus for hemophilia*

4:00-4:15 *Abstract #28:* ***Jing Hu*** *(UPENN) Factor H Host-Recognition Domains Confer Tissue-Specific Protection in Renal and Extrarenal Vascular Beds*

4:15-4:30 *Abstract #29:* ***Vladimir Kolyadko*** *(CHOP) Structural basis for the intrinsic Xase assembly on a procoagulant membrane and the development of factor VIIIa-mediated activity, revealed by cryo-electron microscopy*

4:30-4:45 *Abstract #8: **Connor Watson** (CHOP) Development of a rational engineering approach towards gain-of-function FVIII variants*

4:50-6:00	**Awards Ceremony and Cocktail Reception**

KRB Lobby

Remarks: Amrita Sarkar and Francis Ayombil

Awards announcement by: **Rodney Camire**, PhD, Professor, Endowed Chair in Pediatric, Division of Hematology, Children's Hospital of Philadelphia, University of Pennsylvania & **Lubica Rauova**, MD, PhD,

Associate Professor, Division of Hematology, Children's Hospital of Philadelphia, University of Pennsylvania

Categories include:

- **Top Scoring Abstract**
- **Top Oral Presentation**
- **Top Poster Presentation**

Keynote Speaker Bio



Jorge Di Paola, MD. is the Executive Vice President and Chief Scientific Officer at Versiti. He is the Director of the Versiti Blood Research Institute and Professor of Pediatrics and Associate Dean for Research at the Medical College of Wisconsin. His previous faculty appointments were at the University of Iowa, the University of Colorado and Washington University School of Medicine in St. Louis.

Dr. Di Paola's research focuses on the genetics and biology of bleeding and thrombotic disorders. His laboratory has made significant discoveries in von Willebrand disease, platelet disorders and cancer predisposition. These discoveries have set the stage for potential new therapies. Dr. Di Paola has published more than 200 original scientific articles, reviews and book chapters and is Deputy Editor of the journal *Blood*.

Dr. Di Paola is a past President of the Hemostasis and Thrombosis Research Society (HTRS) and the American Society of Pediatric Hematology Oncology (ASPHO), and past Chair of the 2016 Gordon Research Conference in Hemostasis. Dr. Di Paola has served in multiple National Institute of Health (NIH) study sections and committees.

His awards include the Frank Oski Memorial Lectureship Award from ASPHO, the American Society of Hematology (ASH) mentor award in basic science, the inaugural Arthur Thompson lectureship of the University of Washington, the inaugural Ralph Gruppo lectureship at Children's Hospital Cincinnati and the William Kane endowed lecture at Duke University. Dr. Di Paola is an elected member of the International Society of Thrombosis and Hemostasis (ISTH) Council, the Society for Pediatric Research (SPR), the American Pediatric Society (APS), the Alpha Omega Alpha (AOA), the American Society for Clinical Investigation (ASCI) and the Association of American Physicians (AAP).

Dr. Di Paola has trained more than 30 graduate students, postdoctoral fellows and junior faculty, many of them having their own independent laboratories. Dr. Di Paola's mentoring philosophy is based on transmitting a rigorous and collaborative approach to science with open access to scientific information, always attempting to train the next generation of clinicians and scientists in a multicultural and diverse environment.

Abstracts

ABSTRACT 1:
Platelets increase clot rupture resistance through modulation of fibrin network structure

Rebecca A. Risman[1, 2], Rachel Wernick[2], Daniel Hu[3], Alina D. Peshkova[1], Eva Lungbliudt[2], Rustem I., Litvinov[1], Lauren G. Poole[3,4], Prashant K. Purohit[1], John L. Bassani[1], John W. Weisel[1], Valerie Tutwiler[2]

[1]University of Pennsylvania, Philadelphia, PA, United States, [2]Rutgers University, New Brunswick, NJ, United States, [3]Rutgers Robert Wood Johnson Medical School, Piscataway, United States, [4]Rutgers Center for Environmental Exposures and Disease, Piscataway, United States

Background: Thrombotic embolization is the mechanical rupture or dislodging of an intravascular blood clot (thrombus), resulting in a piece of thrombotic mass (embolus) that can travel through the bloodstream, lodge in downstream vessels, and obstruct blood flow. Despite the life-threatening danger of thrombotic embolization, the mechanisms of this biomechanical phenomenon remain understudied. Previous studies of acellular fibrin clots demonstrated that increasing fibrin densification increased rupture resistance due to a reduction in fluid motion and increase in solid volume fraction; however, the contribution of cells remains unexplored. Therefore, we sought to identify the role that platelets play in altering the mechanical stability (toughness) of fibrin clots.

Methods: We created in vitro tissue factor-triggered clots in human platelet rich (PRP) or platelet-free (PFP) blood plasma. Fracture toughness was determined using experimental force-displacement curves from single-edge notched samples under uniaxial tension. To determine the mechanism of platelet-dependent changes in fracture toughness, we assessed thrombin generation kinetics, degree of fibrin crosslinking using Western blotting, and fibrin network structure using fluorescent confocal microscopy.

Results: Clots formed in PRP were >1.8x resistant to rupture compared to PFP clots. PRP resulted in a higher solid volume fraction and denser fibrin networks due to serum expulsion resulting from platelet-driven clot contraction and compaction. PRP yielded a greater and faster thrombin generation compared to PFP, resulting in more covalent interchain fibrin crosslinking.

Conclusions: An increase in fracture toughness of blood clots by activated platelets may reduce the risk of thrombotic embolization. Our results provide a foundation for future work examining how platelet-driven increases in fracture toughness of blood clots modulate propensity for thrombus rupture

ABSTRACT 2:
Thrombin Induces Rapid Contraction in Hepatic Stellate Cells Driven by PAR1 Signaling

Noah A. Mac,[1] Jordan Lee,[2] Steven An,[1,2] Conor McClenghan,[1,3] Lauren G. Poole[1,4*]

[1]Rutgers University Robert Wood Johnson Medical School, Department of Pharmacology, [2]Rutgers Institute for Translational Medicine and Science, [3]Center of Advanced Biotechnology and Medicine,[4]Rutgers Center of Environmental Exposures and Disease

Background: Clinical and experimental evidence suggests that the coagulation factor thrombin plays a pathologic role in liver fibrosis. One hypothesis linking thrombin to liver fibrosis proposes that thrombin signaling through protease-activated receptor-1 (PAR1) promotes activation of hepatic stellate cells (HSCs), the primary collagen-producing cells in the fibrotic liver. Prior studies report that thrombin promotes HSC contraction in vitro. HSC contraction has been linked to fibrosis by increasing intrahepatic vascular resistance and promoting portal hypertension, as well as inducing mechanosensitive transcription factors involved in HSC activation. This study tests the hypothesis that thrombin-mediated PAR1 activation induces HSC contraction driven by both calcium-dependent (Gq) and –independent (G12/13) signaling pathways.

Methods: Immortalized human HSCs (LX-2) were cultured for 48h then stimulated with human α-thrombin (0.01-1 U/mL) or control. In some experiments, cells were pre-treated with a PAR1 competitive antagonist, vorapaxar (1 μM, VPX), a PAR1-Gq intracellular inhibitor, parmodulin-2 (10 μM, PM2), a Rho kinase inhibitor, Y-27632 (10 μM), or a myosin light chain kinase inhibitor, ML-7 hydrochloride (30 μM) 1h prior to stimulation. Cell contraction was measured using magnetic twisting cytometry. Calcium mobilization and gene expression changes were also assessed.

Results: Thrombin induced rapid cell contraction (within 60 seconds) in a concentration-dependent manner, which was preceded by intracellular calcium mobilization (within 30 seconds). Thrombin-driven contraction and calcium mobilization were completely inhibited by VPX. Inhibition of Gq signaling with PM2 completely suppressed thrombin-driven calcium mobilization and delayed HSC contraction. On the other hand, inhibition of the Rho-ROCK pathway by Y-27632 did not affect thrombin-driven calcium mobilization, but decreased peak HSC contractility. Combined inhibition of Gq and Rho-ROCK signaling completely inhibited thrombin-driven HSC contraction. Mechanical stress has been implicated in HSC transdifferentiation through transcriptional reprogramming. Interestingly, known mechanosensitive differentially expressed genes (DEGs) in HSCs were found to overlap with previously published thrombin DEGs. These DEGs revealed enrichment of biological pathways such as cell migration, adhesion, and angiogenesis. We confirmed that thrombin-driven calcium mobilization (i.e., thrombin:PAR1 signaling) in HSCs was intact after contraction inhibition with ML-7. Based on our previous RNA sequencing results, qPCR analysis confirmed that thrombin induced mRNA expression levels of several DEGs such as CCL2 (Monocyte chemoattractant protein-1), VGLL3 (Vestigial-like family member 3), and GREM1 (Gremlin 1). Interestingly, for CCL2 and VGLL3, both VPX and ML-7 pretreatment blocked the thrombin-driven increase in expression. While for GREM1, only VPX pretreatment blocked the thrombin-driven increase in expression.

Conclusions: These results show that thrombin activation of PAR1 induces HSC contraction both calcium-dependent (Gq) and –independent (G12/13) signaling pathways and upregulates genes known to be associated with mechanosensitive transcriptional reprograming. In conclusion, thrombin may contribute to liver disease pathogenesis by driving HSC contraction to increase portal pressure and regulate transcription. Acknowledgements: Financial support provided by the NIDDK, R00 DK129710, NHLBI, NIH R01HL164404 and P01HL180318, and Rutgers Center for Environmental Exposures and Disease

ABSTRACT 3

Maternal and fetal complications in Obstetric Antiphospholipid Syndrome (OAPS) are Platelet Factor 4 (PF4)-dependent

Diana V. Hnin[1]#, Isabelle Chen[1]#, Preetha Rani Renuka Muthukrishnan[1], Guohua Zhao[1], Jenna Oberg[1], Arin Cox[3], Charles-Antoine Assenmacher[3], Jason Knight[4], Thomas Ortel[5], Keith McCrae[6], Lubica Rauova[1,2], Amrita Sarkar[1,2*], Mortimer Poncz[1,2*]

[1]Division of Hematology, Children's Hospital of Philadelphia, Philadelphia, PA; [2]Department of Pediatrics, Perelman School of Medicine at the University of Pennsylvania, Philadelphia, PA; 3Comparative Pathology Core, Department of Pathobiology, School of Veterinary Medicine at the University of Pennsylvania, Philadelphia, PA, USA; [4]Division of Rheumatology, Department of Internal Medicine, University of Michigan, Ann Arbor, MI, USA; [5]Division of Hematology, Duke University School of Medicine, Durham, NC; [6]Taussig Cancer Institute and Department of Cardiovascular and Metabolic Sciences, Cleveland Clinic Lerner College of Medicine, Cleveland, OH. (#co-first and co-presenting authors).

Background: Antiphospholipid syndrome (APS) is an autoimmune disorder broadly associated with two life-threatening complications: (i) arterial and venous thrombosis and (ii) maternal and fetal injury. We recently reported that β2-glycoprotein I (β2GPI)-specific APS antibodies selectively target PF4:β2GPI:neutrophil extracellular trap (NET) triplexes, such that PF4 is required for APS-associated thrombosis (PMID: 42378231). While thrombosis is a component of OAPS, accumulating evidence suggests that placental injury is also driven by β2GPI and NET-mediated targeting of trophoblastic cells, resulting in inflammation, complement activation, placental dysfunction and adverse pregnancy outcomes.

Aim: We now wish to extend our findings that PF4 is essential for thrombotic complications in APS to the role of PF4 in OAPS using in vitro and in vivo models and to evaluate anti-PF4 blockade as a potential therapeutic strategy in OAPS.

Methods: We used an in vitro BioFlux model with trophoblast cells (HTR-8) to examine trophoblastic dysfunction during APS. The contribution of PF4:β2GPI:NET triplexes to trophoblast injury following addition of IgG from healthy controls (HC) or triple-positive APS patients was evaluated for cellular damage by lactate dehydrogenase (LDH) release, apoptosis by AnnexinV-PI, and downstream inflammatory changes and for PF4 and complement deposition. Protection against these changes by G4KKO, an Fc-modified anti-PF4 antibody, which we have shown prevents APS IgG binding to PF4:β2GPI:NET triplexes, was also assessed.

In vivo studies were performed using a passive immunization model of OAPS. Pregnant mice received either IgG isolated from three triple-positive APS patients (500 μg/mouse) or saline intravenously on gestational day 9 (GD9). Studies were conducted in littermate strains consisting of: (i) murine PF4 knockout (mPF4 KO) mice; (ii) mPF4 KO mice transgenically expressing human PF4 (hPF4); and (iii) hPF4 mice additionally expressing FcγRIIA (hPFm). Outcomes, included maternal weight gain, litter size, fetal growth, and survival to weaning. Placental pathology was evaluated in a blinded manner. Additional studies determined whether G4KKO could prevent OAPS-adverse outcomes.

Results: Only in the presence of both PF4 and β2GPI did APS IgG increase LDH release, indicating trophoblast injury. We did not observe concurrent apoptosis, suggesting cellular dysfunction without overt trophoblastic cell death. Additionally, substantial PF4 and complement deposition on HTR-8 cells supported development of a proinflammatory microenvironment. G4KKO significantly attenuated these effects.

APS IgG induced a robust OAPS phenotype in vivo in hPF4 and hPFm mice that was not seen in the mPF4 KO mice or all three mice phenotypes injected with saline. The hPF4 and hPFm mice post-APS IgG exhibited no maternal weight gain during pregnancy with reduced litter sizes. Fetuses exhibited poor growth at GD17 and, in a separate cohort allowed to undergo natural birth, impaired survival during the first 7 days of life. Disease severity was greater in hPFm mice than in hPF4 mice, suggesting that FcγRIIA-mediated cellular activation contributes to OAPS pathogenesis. Histopathologic examination of placentas from APS-treated hPF4 and hPFm mice demonstrated extensive hemorrhage, fibrin deposition, and tissue necrosis. These findings were absent in APS-treated mPF4 KO mice, whose placentas were indistinguishable from those of saline-treated controls. Therapeutic

intervention with G4KKO significantly reduced placental pathology and reversed maternal and fetal outcomes, maintaining normal physical parameters in both dams and offspring.

Conclusion: We previously showed that PF4 forms an antigenic PF4:β2GPI:NET triplex that is needed to observe APS thrombosis. We now demonstrate, for the first time, a critical role for PF4 in OAPS pathogenesis. In a microfluidic system, PF4 is required as well as ¾2GPI to lead to trophoblastic cell injury. Genetic absence of PF4 protected against APS-induced maternal and fetal injury, whereas expression of human PF4 restored disease susceptibility in both hPF4 and hPFm mice. Blockade of PF4 with the monoclonal antibody G4KKO prevented trophoblastic dysfunction, reduced placental injury, and improved pregnancy outcomes. These findings provide new mechanistic insight into OAPS pathogenesis and identify PF4 as a promising therapeutic target that may complement or potentially replace current non-specific anticoagulant approaches for preventing OAPS

Abstract 4:
A common GRK5 variant enhances PAR1-dependent platelet procoagulant activity and thrombin generation

Hannah Thomson[1], Nina Shaver[1], Xuefei Zhao[1], Francis Ayombil[2], Amrita Sarkar[2], Rodney Camire[2], Mortimer Poncz[2], and Peisong Ma[1]

[1]Thomas Jefferson University, Philadelphia, PA; [2]Children's Hospital of Philadelphia, Philadelphia, PA

Background: Thrombin is a central mediator of hemostasis and thrombosis that activates platelets through the G protein-coupled receptors (GPCRs) PAR1 and PAR4 in humans. We identified a common intronic variant (rs10886430, A G) in G protein-coupled receptor kinase 5(GRK5), homozygous in ~5 million Americans, that reduces GRK5 expression in platelets and enhances PAR1-mediated platelet activation. The variant is associated with an increased risk of venous thromboembolic diseases, including pulmonary embolism (PE) and deep vein thrombosis (DVT). Our prior research demonstrating the near elimination of GRK5 protein expression and platelet hyperactivity to PAR1 agonists in GG individuals was limited to male donors, leaving open the question of whether this phenotype is also present in females. Emerging evidence indicates that platelets are critical initiators and amplifiers of venous thrombus formation by providing procoagulant phosphatidylserine (PS)-rich surfaces that support localized thrombin generation. Importantly, PAR-1 signaling promotes platelet procoagulant activation. However, whether the GG genotype enhances platelet procoagulant activity and thrombin generation remains unknown.

Aim: We hypothesized that the previously identified GG platelet phenotype is conserved in females and that the GRK5 rs10886430 GG genotype enhances PAR1-dependent platelet procoagulant activity and thrombin generation, thereby contributing to venous thrombosis.

Methods: Female AA and GG donor platelets were used to assess GRK5 protein expression through western blotting and platelet reactivity through flow cytometry. Whole blood and washed platelets from human donors with AA and GG genotypes were used to perform thrombin generation assays and to assess procoagulant activity by flow cytometry and a HUVEC-lined microfluidic flow chamber. In vivo thrombosis was evaluated using inferior vena cava (IVC) stasis and PE models in WT and platelet-specific Grk5-/-mice.

Results: Female GG individuals showed a significant reduction in GRK5 expression and increased platelet reactivity to PAR1 agonists, consistent with the phenotype previously observed in male GG donors. Flow cytometric analysis demonstrated that GG individuals displayed an increased percentage of Annexin V+/P-selectin+ procoagulant platelets compared with AA platelets following stimulation with the PAR1 agonist peptide TRAP6, but not the PAR4 agonist peptide AYP, indicating that the GG genotype selectively enhances PAR1-dependent platelet procoagulant activity. GG platelets exhibited increased platelet adhesion and accumulation, PS exposure (Annexin V binding), and fibrin deposition on the hematoporphyrin-injured HUVECs compared with AA platelets. Thrombin generation assays demonstrated that GG platelets generated higher peak thrombin levels than AA platelets following stimulation with either tissue factor (extrinsic pathway) or Actin-FS (intrinsic pathway). To determine whether loss of GRK5 promotes venous thrombosis in vivo, we evaluated PE incidence after IVC stasis assays in platelet-specific Grk5-/- mice. Histological examination of perfused lungs revealed a higher incidence of PE in Grk5-/- mice (83%) compared with WT mice (14%), supporting a role for platelet GRK5 deficiency in promoting venous thrombosis and PE.

Conclusions: The GRK5 rs10886430 GG platelet phenotype is conserved in female donors, extending our previous findings in males. More importantly, these findings demonstrate that the GG genotype enhances PAR1-dependent platelet procoagulant activity and thrombin generation, providing a mechanistic explanation for the increased risk of venous thromboembolism associated with this common variant. These findings further suggest that the GG genotype may serve as a biomarker for identifying individuals at increased risk of venous thromboembolism and may help guide precision antithrombotic therapy.

ABSTRACT 5:

GRK5 and GRK6 play complementary roles in platelet homeostasis by promoting thrombopoiesis and preventing premature platelet clearance

Xuefei Zhao[1], Hannah Thomson[1], Hyun Sook Ahn[2], Christopher Mansi[1], Yanki Yarman[1], Hyunjun Kim[2], Wei Tong[2,4], Timothy J. Stalker[1], Elizabeth Gardiner[3], Mortimer Poncz[2,4], Peisong Ma[1]

[1]Cardeza Foundation of Hematologic Research, Thomas Jefferson University, Philadelphia, PA. [2]Division of Hematology, Children's Hospital of Philadelphia, Philadelphia, PA. [3]John Curtin School of Medical Research, Australian National University, Canberra, Australia. [4]Department of Pediatrics, Perelman School of Medicine, University of Pennsylvania, Philadelphia, PA.

Background: Platelet homeostasis involves a balance between platelet production by megakaryocytes (thrombopoiesis) and platelet clearance. G protein-coupled receptor kinases (GRKs) are serine/threonine kinases that regulate signaling through G protein-coupled receptors (GPCRs) and non-GPCR substrates. We previously demonstrated that GRKs are critical negative regulators of platelet activation. However, the roles of GRKs in MK development and platelet biogenesis remain unknown.

Methods: We generated MK- and platelet-specific double knockouts for GRK5 and GRK6 (*DKO*) in both human and mouse cells. Platelet production and platelet clearance were systematically assessed.

Aims: To define the roles of GRKs in megakaryopoiesis and thrombopoiesis

Results: Compared with Grk5 and Grk6 individual KOs, DKO mice displayed severe thrombocytopenia (~5% of normal platelet counts) and reduced platelet survival. Furthermore, DKO platelets displayed increased integrin activation and granule secretion in both the resting and activated states, which may contribute to their accelerated clearance. However, splenectomy failed to elevate platelet counts in these DKO mice. Bone marrow analysis of DKO mice revealed abnormally shaped MKs clustered near blood vessels, along with myelofibrosis, osteosclerosis, and increased angiogenesis. Plasma levels of TPO and TGF-β1 were 2-3-fold higher in DKO mice than in WT. Transmission electron microscopy demonstrated pronounced alterations in the demarcation membrane system in DKO bone marrow MKs. *Ex vivo* cultured DKO MKs displayed normal size, ploidy, and CD41a+CD42d+ surface expression. Machine learning-assisted image segmentation revealed that DKO MKs had 64% fewer proplatelet-forming MKs, 60% fewer proplatelet tips per cell, and proplatelet tips that were 40% larger compared to WT MKs, suggesting that proplatelet formation was significantly impaired in DKO MKs *ex vivo*. Mechanistically, *Grk5/6*-deficient MKs exhibited elevated RhoA activity, and pharmacological inhibition of ROCK signaling improved proplatelet formation *ex vivo* and partially restored platelet counts *in vivo*. Proteomic and phosphoproteomic profiling of WT and *GRK5/6-/-* human and mouse MKs uncovered glycoprotein (GP) Ibβ as a previously unrecognized candidate non-GPCR substrate and demonstrated that GRK5/6 have a predominant role in regulating key biological processes associated with cytoskeletal remodeling.

Conclusion: We identify GRK5 and GRK6 as dual regulators of platelet homeostasis that promote thrombopoiesis, maintain platelet quiescence, and prevent premature platelet clearance.

ABSTRACT 6:

RepSox Analogs as Potential Therapeutics in RUNX1-Familial Platelet Disorder with Associated Myeloid Malignancy (FPDMM) likely by enhancing RUNX1:CBFβ dimerization

Preetha Rani M.R[1], Rhys Denver[1], Kiwon Lee[2], Shekhar Kumar[1], Paul Liu[3], Alan B. Cantor[4], Samarjit Patnaik[5], Sara E. Kearney[5], and Mortimer Poncz[1,6]

[1]Division of Hematology, Children's Hospital of Philadelphia, Philadelphia, PA; [2]Department of Bioscience and Biotechnology, Hankuk University of Foreign Studies, Yongin, South Korea; [3]National Human Genome Research Center, Bethesda, MD; [4]Division of Hematology Oncology, Boston Children's Hospital, Boston, MA; [5]National Center for Advancing Translational Sciences, Bethesda, MD; Department of Pediatrics, Perelman School of Medicine, University of Pennsylvania, Philadelphia, PA[6]

Background: Familial platelet disorder with associated myeloid malignancy (FPDMM) is caused by RUNX1 haploinsufficiency (RUNX1Lo) and is characterized clinically by defective megakaryopoiesis and platelet (Plt) biology with an increased risk of hematologic malignancies. Our previous studies showed that a small molecule RepSox, initially characterized as an ALK5 inhibitor, improved megakaryocyte (Mk) and Plt biology; however, this activity required high RepSox concentrations (1μM). Also, other ALK5 inhibitors were not effective. We proposed that RepSox may correct Mk and Plt biology by an alternative non-ALK5 pathway.

Aim: To identify and characterize novel RepSox congeners with enhanced potency in RUNX1 haploinsufficient cell models and to investigate their potential mechanism(s) of action.

Methods: Additional RepSox-related compounds were screened for their capacity to correct Mk yield from differentiated RUNX1Lo CD34+-adult hematopoietic stem and progenitor cells (HSPCs) created using lentiviral short hairpin RNA (shRNA) targeting RUNX1 (shRX) or a non-targeting shRNA. 72 hrs after transduction, cells were treated with RepSox or its congeners until differentiated and Mk yield quantified. Lead candidates were then evaluated in iPSC patient-derived cell lines, and in HEL cells. Functional activity was assessed using a c-MPL promoter driven luciferase reporter assay. RUNX1 protein expression level in final Mks was quantified by flow cytometry. Molecular docking analysis using the predictive modelling program, AutoDock Vina v1.2.7, was performed against RUNX1 dimers and RUNX1:CBFβ heterodimers.

Results: Screening identified two RepSox congeners that corrected Mk yield as RepSox, but at lower concentrations and a third that had no efficacy in RUNX1Lo CD34+-cells-derived Mk yield: Compound NCGC00387*472*-01 ("*472*") showed peaked potency at 0.01 μM whereas NCGC00384*167*-02 ("*167*") was active at 500 nM. TPO427*736* ("*736*") was a related RepSox congener that bound as well as RepSox to ALK5 (better than *472* and *167*), but that did not rescue Mk yield and served as a negative control. Both positive congeners also demonstrated efficacy in a patient-derived iPSC line and in HEL cells.

Functional assessment using luciferase reporter system showed that RepSox (1μM), *472* (0.01μM) and *167* (0.5μM) enhanced RUNX1 transcriptional activity by 2.5-fold, 2.6-fold and 1.8-fold, respectively, compared to control. Flow cytometric analysis demonstrated an increase in the RUNX1 protein expression during megakaryopoiesis following treatment with RepSox and with *472* and *167* at their active concentrations. Molecular docking showed weak binding affinity when the three active compounds and the negative control *736* were docked against RUNX1 dimers (ΔG ≈ -6.6 kcal/mol, estimated Kd ≈14.5 μM), but the three active compounds substantially improved interactions with RUNX1:CBFβ heterodimers at a specific pocket. RepSox: ΔG ≈ -7.9 kcal/mol (Kd ≈ 1.6 μM); 472: ΔG ≈ -7.9 kcal/mol (Kd ≈ 1.6 μM); and 167: ΔG ≈ -8.7 kcal/mol (Kd≈ 0.4 μM). The negative control *736* had a ΔG ≈ -6.6 kcal/mol (Kd ≈ 14.7 μM). These data suggest that stabilization of RUNX1:CBFβ heteroduplexes by the small compounds may contribute to their corrective effect on Mk yield in the setting of RUNX1Lo.

Conclusions: We identified two novel RepSox congeners with enhanced improvement in RUNX1 activity in three distinct RUNX1Lo megakaryopoiesis models. Like RepSox but at lower concentrations, compounds *472* and *167* increased cMPL promoter RUNX1 activation and elevated RUNX1 protein expression. Docking studies suggest that interaction with the RUNX1:CBFβ heterodimer may underlie their mechanism of action rather than by inhibiting ALK5 activity. These finding support further preclinical evaluation of these compounds and rationally designing compounds with even greater and specific binding to the identified RUNX1:CBFβ pocket as a potential therapeutic strategy for FPDMM.

ABSTRACT 7:

PF4-Centric Immunothrombotic Disorders Depend on Terminal Complement Activation and Are Responsive to C5 Inhibition

Jenna Oberg[1], Keith McCrae[3], Thomas Ortel[4], Yves Gruel[5], Jerome Rollin[5], Rumi Clare[6], Ishac Nazy[6], Roxanne Cofiell[7], Geoffrey D. Wool[8], Freda Passam[9], Kandace Gollomp[1,2], Douglas B. Cines[10], Gowthami M. Arepally[11], Sung-Kwon Kim[7], Lubica Rauova[1,2], Mortimer Poncz[1,2]*, Amrita Sarkar[1,2]*.

[1]Division of Hematology, Children's Hospital of Philadelphia, Philadelphia, PA; [2]Department of Pediatrics, University of Pennsylvania, Philadelphia, PA; [3]Department of Molecular Medicine, School of Medicine, Case Western Reserve University, Cleveland, OH; [4]Division of Hematology, Duke University, NC; [5]Department of Hemostasis, University Hospital Center of Tours, and UMR INSERM 1327, University of Tours, Tours, France; [6]Department of Medicine, Michael G. DeGroote School of Medicine, McMaster University, Hamilton, ON, Canada; [7]Alexion, AstraZeneca Rare Diseases, New Haven, CT; [8]Department of Pathology, University of Chicago, Chicago, IL; [9]Central Clinical School, Faculty Medicine Health, University of Sydney, Sydney, Australia; [10]Departments of Pathology and Laboratory Medicine and Medicine, University of Pennsylvania, Philadelphia, PA; [11]Division of Hematology, Duke University Medical Center, Durham, NC.

Background: Heparin-induced thrombocytopenia (HIT), vaccine-induced immune thrombotic thrombocytopenia (VITT), and antiphospholipid syndrome (APS) are PF4-centric immunothrombotic disorders characterized by pathogenic antibodies that induce thrombosis through Fc¾RIIA-dependent cellular activation. Our group and others have shown that platelet factor 4 (PF4) bound to von Willebrand factor (VWF) strings and neutrophil extracellular traps (NETs) forms dense antigenic scaffolds that promote pathogenic antibody binding, and platelet and complement activation in HIT and VITT. In APS, β2-glycoprotein I (β2GPI), a known PF4-binding partner, facilitates formation of similar pathogenic antigenic triplexes as we recently reported (PMID:42378231). We hypothesized that terminal complement activation is a shared driver of thrombosis across these disorders and that C5 inhibition would attenuate both thromboinflammatory mechanisms in vitro and disease manifestations in vivo.

Aims: To investigate the role of terminal complement activation in PF4-mediated immunothrombosis and evaluate the effects of C5 inhibition in in vitro and in vivo models of HIT, VITT, and APS.

Methods: Photochemically injured HUVEC-lined microfluidic channels were used to generate VWF strings and adhesion of platelets (Plts) on VWF strings, and complementary neutrophil-based microfluidic systems were used to assess NET-associated thrombosis. Whole blood from healthy donors was incubated with PF4 (25 µg/mL) and purified patient HIT, VITT, or APS IgG (100 µg/mL) with or without eculizumab (10 or 15 µg/mL). Platelet activation, complement deposition, and NET formation were evaluated. The contribution of VWF strings and NETs was investigated using ADAMTS13 and DNase1, respectively. For in vivo studies, Fc¾RIIA+/hPF4+/mPF4−/− (termed as hPFm) mice received anti-mouse C5 antibody BB5.1 (100ug) prior to administration of the HIT-like anti-PF4 monoclonal antibody KKO (1.5µg/g.) Platelet counts and venular neutrophil rolling and thrombosis within cremaster vessels were assessed.

Results: In vitro, eculizumab demonstrated dose-dependent inhibition of PF4-mediated platelet activation. Both 10 and 15 µg/mL eculizumab inhibited HIT and APS-mediated platelet activation, whereas inhibition of VITT-mediated platelet activation was seen at the higher dose. Dose-dependent reductions were observed in complement deposition. Eculizumab (15 µg/mL) inhibited NET formation induced by HIT, VITT, and APS IgG. Furthermore, disruption of VWF strings with ADAMTS13 and degradation of NETs with DNase1 significantly reduced platelet activation, supporting a model in which PF4 bound to VWF strings and NETs serves as critical antigenic scaffolds for pathogenic antibody binding and complement amplification. In the in vivo HIT model in hPFm mice, prophylactic administration of BB5.1 attenuated KKO-induced thrombocytopenia and significantly reduced neutrophil rolling within cremaster venules. BB5.1, both by prophylaxis and therapeutic intervention reduced arterial and venous thrombosis.

Conclusions: PF4-centric immunothrombotic disorders, which now includes APS, share a common pathway in which PF4 bound to NETs or VWF promotes pathogenic antibody binding, complement activation, and thromboinflammatory amplification. In all three disorders, terminal complement inhibition suppresses platelet activation, complement deposition, and NET formation in vitro and protects against thrombocytopenia, vascular inflammation and thrombosis in HIT in vivo. These findings identify C5-dependent complement activation as a

critical therapeutic target in HIT, VITT, and APS and provide a rationale for complement-directed interventions to prevent immunothrombosis.

ABSTRACT 8:
Development of a rational engineering approach towards gain-of-function FVIII variants

Connor T. Watson, Andrew Vanden Heuvel, Anna R. Sternberg, Robert J. Davidson, Johnathan J. Morris, Lindsey A. George

Division of Hematology, Children's Hospital of Philadelphia, Philadelphia, PA.

Background: In recent years, gene therapy has emerged as a viable treatment for numerous genetic disorders that are difficult to address by conventional therapeutic avenues. Of these, hemophilia A (HA) is a particularly attractive candidate due to a single encoding gene for FVIII, the high tropism of AAVs for liver tissue where FVIII is produced, and immunogenic complications with plasmapheresis. Despite this, concerns of low levels of expression and poor durability of first-generation gene therapies highlight a need for gain-of-function (GOF) FVIII variants to expand the therapeutic window. While thousands of unique HA-causing mutations exist, the most common is intron 22 inversion, accounting for 40-50% of severe cases. Concomitant disruption of exons 23-26 results in dysfunctional C1 and C2 domains that interfere with vWF and membrane binding, both of which are essential for extending the half-life of FVIII and maintaining function. As part of a broader gene-editing approach to correcting this mutation, a rational engineering approach was employed to develop GOF FVIII variants with mutations in regions of the C1 and C2 domains.

Methods: FVIII exons 23-26 were screened for target residues that demonstrated conservation between species, were not linked to known HA mutations, and were expected to have a functional role in membrane binding (Pellequer et al., 2011, Avery et al., 2025). Mutations at these residues were designed to enhance electrostatically favorable interactions with anionic phospholipid membranes. Mutant plasmids were commercially obtained, and Huh7 cells were transiently transfected and screened by one-stage assay (OSA) and ELISA. After screening, a selected GOF variant was stably expressed in BHK cells and purified. The recombinant protein was biochemically characterized and used to perform a tail-clip assay and a modified *in vivo* model of femoral vein thrombosis sensitive to elevated FVIII levels (Gollomp et al., 2018, Welsh et al., 2019) in immune compromised hemophilia A (HA/CD4KO) mice. Briefly, mice were injected with fluorescent markers for platelets and fibrin diluted in PBS with recombinant FVIII at either 100% or 500% of normal antigen levels. Endothelial injury was induced by tissue paper soaked in 2% $FeCl_3$ in contact with the exposed femoral vein for 5 minutes. Thrombus growth was then monitored by intravital confocal microscopy for 30 minutes.

Results: Screening of transiently transfected cells yielded two GOF C2 domain variants (>2-fold improvement of specific activity over FVIII-SQ control), L2251K and L2252K. L2252K was purified, with the recombinant protein demonstrating 1.6-fold higher specific activity by OSA (17000 IU/mg v. 11000 IU/mg) over recombinant FVIII-SQ. Intrinsic Xase assays displayed roughly 2-fold enhanced function of the intrinsic Xase complex with no distinct increases in FX or FIXa affinity. In a tail clip bleeding challenge, L2252K corrected at half the required dose of FVIII-SQ (6 ug/kg v. 12 ug/kg). In a model of femoral vein thrombosis, L2252K and FVIII-SQ injected at 100% antigen levels did not display significantly elevated platelet or fibrin accumulation over WT controls. Positive controls with known thrombogenic phenotypes (homozygous Factor V Leiden mice and 500% antigen FVIII-SQ) displayed significantly elevated platelet and fibrin accumulation over WT controls and 100% levels of both recombinant FVIII-SQ and L2252K.

Discussion: A rational engineering approach was employed towards the development of a gain-of-function FVIII C2 domain variant. This study validated the use of selection criteria based on species homology, lack of association with HA-causing mutations, and structure-informed functional consequences. The swap of these target residues towards charge-favorable mutants enhanced FVIII function in both transient transfections and as a recombinant protein. The purified GOF variant displayed improved hemostatic ability in an *in vivo* bleeding challenge and no apparent pathological thrombogenicity in a model of venous thrombosis. This study is a first step in an overarching approach towards a rationally engineered GOF FVIII variant with translational potential for gene-therapy directed rescue of the HA-causing intron 22 inversion.

ABSTRACT 9:
Elevated Factor VIII activity is an independent risk factor for venous thrombosis.

Johnathan J. Morris,[1,2] Connor T. Watson,[1,2] Robert J. Davidson,[1] and Lindsey A. George[1,2]

[1]Perelman Center for Cellular and Molecular Therapeutics and Hematology, Children's Hospital of Philadelphia, Philadelphia, PA, United States; [2]Department of Pediatrics, Perelman School of Medicine, University of Pennsylvania, Philadelphia, PA, United States

Background: Elevated Factor VIII (FVIII) activity is an established risk factor for venous thrombosis (VT), with VT risk exceeding all other procoagulant factors, except von Willebrand Factor (vWF). However, because FVIII circulates in a high-affinity complex with vWF, and both proteins are elevated during physiologic stress, it remains unclear whether elevated FVIII activity independently promotes VT or primarily reflects an underlying inflammatory state. Consistent with epidemiologic data, naturally occurring human FVIII variants, including FVIII Padua and the recently described FVIII Aurora, demonstrate that elevated FVIII activity due to increased expression or enhanced potency, respectively, is associated with thrombosis despite physiologic vWF levels. Despite these observations, the biochemical mechanisms linking elevated FVIII activity to VT remain unclear. We therefore investigated the procoagulant effect of elevated FVIII in plasma compared to equal-fold increases in FIX and FV and the prothrombotic potential of elevated FVIII in hemophilia A (HA) mice with and without vWF deficiency.

Methods: Pooled normal human plasma (NHP) was supplemented with (r)ecombinant FVIII, FIX, or FV to achieve 1–10-fold normal levels and coagulation was initiated with tissue factor. Thrombin, FIXa, and FXa generation with increased FVIII was compared to equal-fold increases in FIX, an established independent VT risk factor, and FV, which is not associated with increased VT risk. FIXa and FXa generation were measured by ELISA-based quantification of FIXa-antithrombin (AT) and FXa-AT complexes. The in vivo prothrombotic potential of elevated FVIII activity was assessed in HA and HA/vWF deficient (HA/vWF-/-) mice using a ferric chloride-induced femoral vein thrombosis model. Mice were infused with rFVIII to achieve 0%, 30%, 100%, or 500% of normal FVIII activity. Platelet and fibrin accumulation were quantified by intravital confocal microscopy. Thrombus formation was compared with homozygous FV-Leiden (FVL+/+) mice, which have a robust prothrombotic phenotype. To additionally isolate the contribution of FVIII from vWF, HA mice were infused with FVIII-Y1680F, which has ≥10-fold reduced vWF binding efficiency.

Results: Increasing concentrations of FVIII and FIX in NHP enhanced thrombin, FIXa, and FXa generation in a dose-dependent manner. Equal-fold increases in FVIII and FIX concentrations produced similar peak thrombin and endogenous thrombin potential, while elevated FVIII produced shorter lag times at higher factor concentrations, suggesting more rapid propagation of coagulation. Ten-fold normal FVIII concentrations resulted in FIXa and FXa generation of 200% and 170% of NHP, respectively, while 10-fold normal FIX concentrations resulted in FIXa and FXa generation that was 160% and 120% of NHP, respectively. In contrast, 1–10-fold normal FV concentrations produced no appreciable change in thrombin, FIXa, or FXa generation. In HA mice, increasing FVIII activity produced dose-dependent increases in platelet and fibrin accumulation following femoral vein injury. HA mice with 100% FVIII activity restored thrombus formation to that of WT mice. HA mice with 500% FVIII activity exhibited platelet and fibrin accumulation that was 6-fold and 3-fold greater than that of WT mice, respectively, producing a prothrombotic phenotype indistinguishable from FVL+/+ mice ($P < 0.1246$ and $P < 0.5557$, respectively). Importantly, the prothrombotic effect of elevated FVIII was preserved in HA/vWF-/- mice. HA/vWF-/- mice with 500% FVIII activity exhibited 4-fold greater platelet and 2-fold greater fibrin accumulation over HA/vWF-/- mice with 100% FVIII activity. Similarly, HA mice with 500% FVIII-Y1680F activity exhibited platelet and fibrin accumulation comparable to HA/vWF-/- mice with 500% FVIII-WT activity, further supporting that increased thrombus formation due to elevated FVIII activity is independent of vWF.

Conclusions: By directly comparing equal-fold increases in FVIII, FIX, and FV, these studies demonstrate that FVIII disproportionately amplifies coagulation relative to equal-fold increases in FIX and FV. Our in vivo studies demonstrate that elevated FVIII activity is sufficient to drive venous thrombosis independent of vWF, supporting FVIII as an independent mechanistic driver of VT rather than a biomarker of inflammation. These findings provide a mechanistic explanation for longstanding epidemiologic observations linking elevated FVIII to VT.

ABSTRACT 10:
Hemostasis is potentiated during local LPS exposure mimicking pathogen invasion

Jenna R. Severa, Christopher D. Mansi, Brenna B.Y. Mathers, Lauren M. Berish, and Timothy J. Stalker.

Cardeza Foundation for Hematologic Research, Department of Medicine, Thomas Jefferson University, Philadelphia, PA, USA, 19107

Introduction: Hemostasis is the physiologic process of clotting in response to vascular injury. Such injuries present an opportunity for exposure to pathogens, which would require an immune response alongside the hemostatic response to both successfully stop bleeding and prevent infection. Therefore, hemostasis can be viewed as a first step in addressing pathogen exposures at sites of vascular injury. We hypothesized that the platelet/thrombin/immune cell axis, including Par4 signaling, regulates hemostasis in the context of pathogen invasion.

Methods: The hemostatic response was studied using a jugular vein puncture injury model in male and female mice. Lipopolysaccharide (LPS, 2 µg/mL) was applied to the jugular vein topically after hemostasis was achieved to mimic pathogen invasion. C57BL/6J mice were used to study the effects of pathogen invasion during initial hemostasis. Anti-P-selectin function-blocking antibody was used to study the role of leukocyte recruitment in pathogen invasion during hemostasis. LysMCre$^{+/+}$Par4$^{fl/fl}$ and Pf4Cre^{+}Par4$^{fl/fl}$ mice were used to study the role of leukocyte and platelet Par4 signaling, respectively. Hemostatic plugs were imaged using tissue-cleared confocal microscopy, and platelet plug volume, fibrin deposition, platelet activation status, and neutrophil recruitment were quantified.

Results: In response to topical LPS administration, platelet plug volume, dense platelet region (DPR) volume, and fibrin deposition were significantly increased compared to saline-treated controls ($p = 0.04$, $p = 0.03$, and $p = 0.04$, respectively, n = 7-8/group.) To determine if these changes were mediated by immune cells, we utilized a P-selectin function-blocking antibody to block immune cell recruitment to hemostatic injury sites. Blockade of P-selectin successfully abrogated neutrophil recruitment in the context of LPS treatment. Furthermore, blockade of leukocyte recruitment reduced platelet plug volume and fibrin deposition within the DPR ($p = 0.01$ and $p = 0.04$, respectively, n = 12/group). To investigate the role of leukocyte Par4 signaling in this context, we utilized a leukocyte-specific knockout of Par4 (LysMCre$^{+/+}$Par4$^{fl/fl}$). Par4 knockout on leukocytes did not alter platelet plug volume or endothelium neutrophil recruitment; however, a small but significant reduction in plug-associated neutrophil recruitment was observed ($p = 0.02$, n = 16-19/group). In the context of LPS treatment platelet Par4 knockout mice (Pf4Cre^{+}Par4$^{fl/fl}$) had no difference in platelet activation or fibrin formation as compared to controls, although Par4 knockout mice did exhibit modestly smaller platelet plugs overall. Interestingly, platelet-Par4 knockout mice undergoing the pathogen invasion model exhibited no rebleeding, which is normally observed in Par4 knockout mice at the same injury size in sterile context. Platelet Par4 signaling was also dispensable for neutrophil recruitment in this context.

Conclusions: Taken together, our data demonstrate that LPS treatment potentiates the hemostatic response in a leukocyte-dependent manner that is independent of Par4 signaling. Future studies will investigate the apparent leukocyte mediated mechanism driving increased platelet activation and fibrin deposition.

ABSTRACT 11:
PAD4 deficiency increases APAP-induced liver injury independent of NET formation

Gina E. Capece,[1] Sara Calvo Londono,[1] Amish K. Patel,[1] Robert A. Campbell,[2] James P. Luyendyk,[3] Lauren G. Poole[1,4]

[1]Rutgers University Robert Wood Johnson Medical School, Department of Pharmacology; [2]Washington University, Department of Emergency Medicine; [3]Department of Pathobiology and Diagnostic Investigation, Michigan State University; [4]Rutgers Center for Environmental Exposures and Disease. RWJMS Research Tower Room 514, Piscataway, NJ 00854 Phone: 732-235-9363, email: gc679@rutgers.edu

Background: Overdose on the over-the-counter pain medication acetaminophen (APAP) is the leading cause of drug-induced acute liver injury (ALI) in the United States.

Experimental evidence suggests that neutrophils contribute to liver damage in experimental APAP-induced acute liver failure (ALF). One potential mechanism whereby neutrophils may promote liver injury is through the formation of neutrophil extracellular traps (NETs). NETs are extracellular networks comprised of DNA, histones, and neutrophil proteins (e.g. myeloperoxidase (MPO), elastase). Routinely used biomarkers of NETs are increased in the blood and livers of patients with APAP-induced ALF; however, the precise contribution of NETs to APAP-induced ALI and ALF is unclear.

Aim: We sought to characterize NET formation over time in experimental ALI and ALF and determine the role of NET formation in liver damage after APAP challenge.

Methods: 8-week-old male wildtype mice were fasted overnight and challenged with APAP to induce ALI (300 mg/kg) or ALF (600 mg/kg) or given vehicle (saline). To determine the impact of neutropenia on APAP-induced liver injury, mice were administered a neutrophil-depleting antibody (50 µg anti-Ly6G isotype, clone 1A8, i.p.) or isotype control 24 h prior to APAP challenge. We also determined the impact of deficiency in peptidyl arginine deiminase-4 (PAD4), an enzyme critical for NET formation, in APAP-challenged mice by comparing wildtype mice (PAD4+/+) to PAD4-deficient mice (PAD4-/-).

Results & Conclusions: APAP challenge at both doses caused robust hepatocellular necrosis that increased in a time-dependent manner in wildtype mice. APAP challenge caused time-dependent infiltration of intrahepatic PAD4+ neutrophils (PAD4+Ly6G+ cells). Interestingly, PAD4+ neutrophil infiltration was significantly higher in the ALI group compared to ALF ($p=0.0031$). Despite abundant infiltration of PAD4+ neutrophils, intrahepatic NETs (Ly6G-CitH3-DAPI+ cells) were extremely rare in all treatment groups. We next measured levels of two routinely used biomarkers of NETs in plasma: MPO-DNA complexes and citrullinated histone 3 (CitH3) nucleosomes. Plasma MPO-DNA complex levels were near or below the limit of detection in all samples, except in the ALI group at 12 hours after APAP challenge. In contrast, CitH3 nucleosomes were significantly increased at both 6 h and 12 h after APAP challenge in both the ALI and ALF groups ($p<0.001$).

Intrahepatic NETs, though rarely detected in APAP-challenged PAD4+/+ mice, were not observed in APAP-challenged PAD4-/- mice. Importantly, levels of plasma CitH3 nucleosomes in APAP-challenged mice were unaffected by either PAD4 deficiency or neutrophil depletion, indicating that plasma CitH3 nucleosomes do not reflect NETs in this experimental context. Finally, we sought to investigate the role of NETs in APAP-induced ALI and ALF. Remarkably, and in contrast to the protective effect of neutrophil depletion on APAP-induced ALF, PAD4 deficiency produced dramatic mortality (~60%), exacerbated liver necrosis (1.2-fold increase, $p=0.09$), and hepatic vascular congestion and hemorrhage (2.3-fold increase, $p=0.008$) in APAP-induced ALF. Taken together, the results indicate that PAD4 plays a hepatoprotective role in APAP overdose by a mechanism independent of NET formation. Furthermore, our results strongly suggest that context-dependent validation of common NET biomarkers is essential, particularly in experimental settings of acute liver injury.

ABSTRACT 12:
Effects of Mechanical Tension on Structural and Biochemical Regulation of Fibrinolysis

Eva Iungbliudt[a,b], and Valerie Tutwiler[a]

[a]Department of Biomedical Engineering, Rutgers University, Piscataway, NJ, USA; [b]Department of Chemical and Biochemical Engineering, Rutgers University, Piscataway, NJ, USA

Fibrinolysis is the proteolytic degradation of fibrin fibers, the main structural and mechanical component of blood clots. Fibrinolysis is primarily regulated by plasmin, which is activated from its zymogen plasminogen by tissue-type plasminogen activator (tPA) that noncovalently binds to fibrin. Blood clots are subjected to mechanical tension from the blood flow, clot contraction, and pulsatile vessel wall motion. Despite the pathophysiological relevance of mechanical forces, the interplay between fibrin mechanics and plasmin-mediated lysis remains understudied. Mechanical stress can trigger changes in the fibrin network structure, the biochemical microenvironment, and protein transport within the network. An increase in tension, as occurs with clot contraction, has been shown to differentially modulate fibrinolysis. There is conflicting evidence regarding whether mechanically strained fibrin accelerates or attenuates fibrinolysis; hence, the mechanisms by which mechanical tension influences fibrinolysis remain poorly understood. Thus, we aim to investigate the role of mechanical tension in the regulation of fibrinolysis.

To determine how mechanical tension influences internal fibrinolysis, we utilized commercially available citrated platelet-poor plasma (Cone Bioproducts). The effects of tension were evaluated using a combination of assays, including uniaxial mechanical testing, turbidity, and ELISA. The samples were formed in custom-fabricated 20 × 20 × 2 mm molds previously coated with 4% Triton X-100. Samples were activated (15 pM tissue factor and 25 mM CaCl2) allowed to polymerize for 15 minutes to ensure full clot formation and FXIIIa-mediated crosslinking. When applicable, tPA was added before clotting. Following polymerization, fibrin gels were immediately transferred and mounted on the mechanical tester using rectangular clamps. Uniaxial tension was applied to the sample at a strain rate of 0.1 mm/s to reach fixed strains (5%, 25%, 50%, or 75%) to simulate different degrees of mechanical tension, and the strain was maintained throughout the experiment.

Mechanical testing results showed a nonlinear increase in force with increasing strain, reflecting the stiffening of fibrin fibers, with the maximum force reached at 75% strain ($p < 0.0001$). The time to full lysis was observed to be insignificantly different across the strains ($p > 0.05$). However, the rate of lysis, defined as the slope of a change in force over time, increased with the increasing strain ($p < 0.01$). The SEM analysis revealed fibrin network rearrangements under tension and more pronounced fiber realignment and bundling as strain increased ($p< 0.0001$); however, the single-fiber diameter was found to be strain-independent ($p > 0.05$). Moreover, application of strain resulted in the expulsion of serum, which was later analyzed for the presence of pro- and anti-fibrinolytic agents using ELISA. Immunosorbent assays of profibrinolytic enzymes in serum showed greater tPA expulsion at lower strain; however, plasminogen release was strain-independent. Analysis of antifibrinolytic enzymes showed increased PAI-1 and decreased TAFI expulsion under higher strain. D-dimer ELISA of the clot lysate showed a 2.1-fold increase in D-dimer release at later lysis timepoints in highly-strained clots.

Together, our current results indicate that applied tension affects fibrinolysis through a variety of mechanisms, including structural rearrangement of the fibrin network via bundling and alignment, as well as modulation of the biochemical environment of the clot via expulsion/retention of certain fibrinolytic regulators. These findings suggest that accounting for the mechanics and morphology of a blood clot may therefore be important for understanding variability in fibrinolytic treatment response and may aid in developing more effective, individualized therapeutic strategies.

ABSTRACT 13:
Regulatory Control of FV-Short Splicing by F5 Exon 13

Alice M. Todaro, PhD[1], Matthew W. Bunce, PhD[1], Francis Ayombil, PhD[1], Jordan Ulsh[1], Jacinta Davis, PhD[2], Andrei Thomas-Tikhonenko, PhD[2,3], Rodney M. Camire, PhD[1,4]

[1]Division of Hematology and the Raymond G. Perelman Center for Cellular and Molecular Therapeutics, The Children's Hospital of Philadelphia, Philadelphia, PA; [2]Department of Pathology and Laboratory Medicine, University of Pennsylvania, Philadelphia, PA; [3]Division of Cancer Pathobiology, Children's Hospital of Philadelphia, Philadelphia, PA; [4]Department of Pediatrics, Perelman School of Medicine, University of Pennsylvania, Philadelphia, PA

Background: Factor V (FV) plays a central role in coagulation through both pro- and anticoagulant functions. Alternative splicing within exon 13 of the *F5* gene, produces FV-short, a physiologic isoform that binds with high affinity to tissue factor pathway inhibitor alpha (TFPIα), increasing TFPIα stability and anticoagulant activity. Under normal conditions, FV-short is produced at very low concentrations (~0.2–0.5 nM), reflecting tight control of its splicing. However, certain genetic variants disturb this balance. FV-East Texas mutation strengthens the alternative donor site, increasing FV-short and causing disproportionate TFPIα elevation and bleeding disorder. FV-Atlanta, characterized by an 832-bp deletion within exon 13, leads to extremely high FV-short concentrations (~30–40 nM) and results in severe bleeding. These findings suggest loss of splicing regulatory elements (SRE) that normally suppress FV-short splicing. However, the underlying mechanisms remain unknown.

Aim: To define the molecular mechanisms regulating FV-short splicing.

Methods: Minigene constructs containing either wild-type exon 13 (FV-WT) or the FV-Atlanta deletion (FV-ATL, Δ832 bp), flanked by partial intronic sequences, were generated to evaluate exon 13 splicing and define the regulatory role of the deletion. Constructs were transfected into Expi293 cells, followed by RNA isolation, RT-PCR amplification, and electrophoretic analysis of splice products.

Results: the FV-WT minigene predominantly produced full-length exon inclusion with minimal FV-short splicing. In contrast, FV-ATL showed markedly increased FV-short splicing and reduced use of the canonical intron-exon junction. To further validate the model, FV-short donor and acceptor splice sites were strengthened. While strengthening the alternative donor (FV-East Texas) increased FV-short splicing as expected, enhancing the alternative acceptor in both FV-WT and FV-ATL similarly upregulated FV-short.

To identify the regulatory region controlling FV-short expression, defined portions of the Atlanta deletion were systematically reintroduced into the FV-ATL construct. This resulted in the identification of an SRE of <200-bp that strongly suppressed FV-short production and restored canonical splice-site usage. Similar results were observed using full-length *F5* cDNA constructs and across multiple cell lines. To confirm sequence specificity, the <200-bp region was replaced with either scrambled sequence or an unrelated insert (*F8* sequence), neither of which reduced FV-short expression. In addition, to determine whether the identified suppressor region in exon 13 was *F5*-specific, the SRE was inserted into an unrelated gene (*F10*). The introduction of the SRE in intron 4 of *F10* resulted in splicing suppression, in contrast to normal intron 4 splicing observed in *F10* wild-type.

Conclusions: We identify a previously unrecognized specific *cis*-regulatory element within exon 13 restraining FV-short splicing. Our findings demonstrate that multiple sequence alterations within exon 13 of *F5* including deletions or splice-site-strengthening mutations can modulate FV-short expression, thereby shifting anticoagulant activity and influencing normal hemostasis. Importantly, the identified SRE is able to function as splicing suppressor in a separate gene (*F10*), showing its potential to modulate splicing beyond *F5*.

ABSTRACT 14:
Platelet-Lymphocyte Ratio (PLR) as a Predictor of Mortality in Severely Injured Patients

Zachary Cartnick, Gina Vargas, Andrew Gosselin, Valerie Tutwiler, Julie Goswami

Introduction: Early changes to normal blood clotting and the immune response to traumatic injury are believed to be intricately linked. There are however limited available biomarkers of this trauma-induced immune-coagulopathy that can be used to predict and stratify outcomes, including mortality, thromboembolic events, and infectious complications. Pre-clinical studies have demonstrated a potential role of more specific markers of clotting kinetics and mechanics as predictors of adverse outcomes after injury, but these biomarkers are not yet readily available. Admission complete blood counts (CBC)provide white blood cell count with differential, hemoglobin and hematocrit, and platelet counts. No one value from CBC or single static coagulation test (partial thromboplastin time, prothrombin time) has been consistently associated with clinical phenotype or outcome. However, prior studies have shown potential link of admission platelet-lymphocyte ratio (PLR), a readily accessible biomarker derived CBC, to injury severity, transfusion needs, and mortality after traumatic injury. In this study, we evaluate the impact of clinical factors (age, injury severity score) on admission PLR as well as the potential for PLR as a predictor of mortality in severely injured adult patients.

Methods: This is a single center retrospective study at our Level 1 Trauma Center and approved by our Institutional Review Board. Patients eligible for the study were identified using our institutional Trauma Registry. Patients 18 years of age and older, who presented as trauma activations in 2024 or 2025 with ISS 25 or higher were included. Patients were excluded from the study if they did not have a complete blood count with differential within 24 hours of admission or if they had known pre-hospital anticoagulant use or bleeding/clotting disorder. Chart review of admission laboratory values was performed using the electronic medical record. Our primary outcome was mortality. Data analysis was performed using GraphPad Prism 10. All variables are expressed as median with quartiles [Q1, Q3] or as absolute number or percent of whole. Mann-Whitney U test used for comparison of continuous variables. Univariable and multiple variable logistic regression for predictive models. $P < 0.05$ considered statistically significant.

Results: A total of 194 patients were included in this study with median age 52 [34, 70] and median ISS 27 [26, 34]. Of the included patients, 69.1% (n = 134) were male and the majority (91.8%) suffered blunt mechanism injury. There were a total of 35 (18.0%) mortalities and 8 (4.1%) patients suffering thrombotic events, including venous thromboembolism and pulmonary embolism. In comparing patients who died vs. those who survived, patients who died were of comparable age (54 [32, 69] vs. 52 [34, 71], $p = 0.775$) and comparable injury severity score (ISS) (29 [26, 35] vs. 27 [26, 34], $p = 0.117$). In comparing laboratory values by mortality, patients who died had comparable platelet counts (154 [121, 203] vs. 155 [108, 250], $p = 0.106$), comparable absolute lymphocyte counts (1.2 [0.8, 2.6] vs. 1.1 [0.7, 1.8], $p = 0.163$), but decreased PLR (133.2 [78.9, 201.8] vs. 162.9 [114.7, 275.4], $p = 0.016$) in comparison to those who survived. PLR showed a weak positive correlation to chronologic age in years ($R^2 = 0.022$, $p = 0.039$) but no significant correlation to ISS. Based on this we performed univariable receiver operating characteristic (ROC) analysis of PLR ratio as a predictor of mortality and were able to identify an optimal cutoff of 113.6 ($p < 0.017$) with specificity of 75%. Using this cutoff, lower PLR showed a statistically significant association with admission Glasgow Coma Scale (GCS) but not with age or ISS. Finally, in this cohort, a multiple variable model using age and ISS only was not predictive of mortality. Adding PLR to the model resulted in statistical significance with area under ROC curve 0.638 ($p = 0.011$). The multiple variable model was further strengthened by adding GCS with area under ROC curve for the four variable model 0.832 ($p < 0.001$).

Conclusion: Admission PLR, an easily and immediately obtainable biomarker representing the interface between coagulation and inflammation, shows promise for prediction all-cause mortality in severely injured trauma patients, in both univariable and multivariable models, and exhibits age-associated variability.

ABSTRACT 15:
Mechanistic Analysis of Coagulation Factor V Anticoagulant Function in APC Sensitivity

James Bachman[1,2], Matthew W. Bunce[2], Francis Ayombil[2], and Rodney M. Camire[2,3] [1]Department of Chemistry, College of Arts and Sciences, University of Pennsylvania, Philadelphia, PA

[2]Division of Hematology and the Raymond G. Perelman Center for Cellular and Molecular Therapeutics, The Children's Hospital of Philadelphia, Philadelphia, PA [3]Department of Pediatrics, Perelman School of Medicine, University of Pennsylvania, Philadelphia, PA

Background: Factor V (FV) plays a central role in coagulation as it potentiates thrombin generation upon its proteolytic activation to FVa. FV also has anticoagulant function serving as a cofactor for activated protein C (APC) in the proteolytic inactivation of factor VIIIa (FVIIIa). We investigated how factors such as FXa binding, APC sensitivity of FVIIIa, and FV cleavage state influence this anticoagulant activity using engineered FV-short variants in plasma-based clotting assays.

Methods: Activated partial thromboplastin time (aPTT) assays were performed in pooled normal plasma or FVIII-deficient plasma reconstituted with recombinant proteins. APC sensitivity was quantified in these experiments using the APC sensitivity ratio (APCsr; clotting time with APC / clotting time without APC). For these studies we employed a naturally occurring FV splice variant, FV-short, containing mutations that eliminate binding to FXa without compromising its APC cofactor function, thereby decoupling its procoagulant and anticoagulant functions. Dependence on FVIIIa inactivation was assessed by comparing wild-type B-domainless FVIII (FVIII-SQ) and APC-resistant FVIII (FVIII-QQ) in aPTT assays with this FV-short Xa mutant (FVs-AC; anticoagulant only). Since conversion of FV to FVa alters its ability to function within the APC anticoagulant pathway, we then tested whether thrombin-mediated cleavage of both FVs-AC and a thrombin-resistant version of FV-AC (FVs-AC-QQ) altered its APC-enhancing activity within aPTT assays.

Results: In the absence of APC, increasing concentrations of FVs-AC had a minimal effect on clotting time in PNP. When 60 nM APC was added to normal plasma, clotting times were prolonged in correlation with increasing variant concentration, with the APCsr value increasing from 3.9 at 0 nM to 5.4 at 200 nM FVs-AC concentration. These results indicate that FVs with only anticoagulant properties enhances APC-dependent anticoagulant activity without altering baseline coagulation, making it a viable tool in further studying FV anticoagulant function. In FVIII-deficient plasma, FVs-AC demonstrated the strongest anticoagulant effect on clotting times when plasma was reconstituted with FVIII-SQ. In contrast, reconstitution with FVIII-QQ reduced this effect with a more modest increase in the APC sensitivity ratio. Pre-cleavage of FVs-AC with thrombin reduced its APC-enhancing effect, lowering the APCsr value from 6.5 to 3.4. Thrombin-resistant FVs-AC-QQ, in comparison, maintained anticoagulant activity in aPTT assays before or after thrombin treatment, with only a modest decrease in APCsr from 6.6 to 5.7.

Conclusion: These results demonstrate FV/FV-short enhancement of FVIIIa inactivation by APC-dependent anticoagulant effects using a clinically relevant assay for assessing APC resistance. The loss of FVs-AC APC cofactor activity upon thrombin cleavage further demonstrates how proteolytic processing of FV/FV-short modulates its APC cofactor function. Overall, these findings help define the functional requirements that regulate FV anticoagulant activity. Future studies utilizing thrombin generation assays will help to determine how these changes in APC sensitivity influence thrombin generation beyond endpoint clotting measurements.

ABSTRACT 16:
GRK Inhibition enhances platelet reactivity in a microfluidic model of acquired hemophilia

Brenna B.Y. Mathers, Meghan E. Roberts, Scott L. Diamond, Peisong Ma, Timothy J. Stalker

Cardeza Foundation for Hematologic Research, Department of Medicine, Thomas Jefferson University, Philadelphia, PA 19107

Background: G protein-coupled receptor kinase 5 (GRK5) signaling negatively regulates platelet responsiveness to thrombin via PAR1 in humans. Consequently, individuals with a GRK5 polymorphism that results in reduced GRK5 levels are more likely to experience thrombotic events compared to those without. Here, we're exploring whether this interaction is relevant in the context of coagulation deficiencies when thrombin activity is reduced. Our lab has previously shown that loss of thrombin-mediated platelet activation is a major factor contributing to increased bleeding in murine hemophilia models. We hypothesized that GRK inhibition in a microfluidic model of acquired hemophilia would increase platelet sensitivity to thrombin to recover platelet activation.

Methods: We utilized a custom microfluidic model using healthy human donor blood flowed over a collagen and tissue factor coated surface at venous shear (200 s^{-1}). Over multiple experiments, the blood was incubated individually with a variety of treatments, including PAR1 and PAR4 antagonists (vorapaxar and BMS-986120, respectively), a pan GRK antagonist (CCG-215022), and a FVIII neutralizing antibody (FVIII nAb, GMA-8015) and compared to the respective vehicle controls. Fluorescent labeling was used to image platelets (hCD41), procoagulant platelets (annexin V), P-selectin surface expression, and fibrin over time.

Results: In normal healthy donor blood, PAR1 antagonism resulted in reduced total platelet accumulation and fibrin deposition compared to the vehicle control group (47% and 32% of control, $p<0.0001$ and $p=0.0006$, platelets and fibrin respectively). PAR4 antagonism specifically reduced procoagulant platelet activation as measured by annexin V labeling to 74% of the vehicle control group ($p=0.0009$). These results indicate that our model is sensitive to thrombin-mediated PAR activation.

Pan GRK inhibition substantially increased procoagulant platelets to 154% of the vehicle control group ($p=0.0244$) and modestly increased platelet accumulation and fibrin deposition. With the assay conditions used, inhibition of FVIII activity reduced platelet accumulation and activation by more than 50% ($p<0.0001$ and $p=0.0113$, respectively), and completely abolished fibrin formation. When FVIII activity and GRKs were inhibited simultaneously, GRK antagonism moderately increased platelet accumulation and recovered procoagulant platelets to control levels as compared to FVIII inhibition alone ($p=0.0198$ vehicle vs FVIII nAb alone, and $p=0.0170$ FVIII nAb alone vs FVIII nAb + CCG-215022). Additionally, when labeling P-selectin to analyze platelet ¾-granule release, P-selectin positive platelets were reduced by about half during FVIII inhibition alone, but were recovered to 78% of control during simultaneous FVIII and GRK inhibition ($p = 0.0004$, $p = 0.0351$, vehicle vs FVIII nAb alone and FVIII nAb alone vs FVIII nAb + CCG-215022, respectively).

Conclusion: Our findings demonstrate that GRK inhibition increases platelet reactivity in the context of coagulation deficiency and suggest that increasing platelet sensitivity to thrombin may be an effective therapeutic strategy in treatment of bleeding disorders.

ABSTRACT 17:

A reproducible peel testing platform for quantifying adhesive strength at the blood clot - vessel wall interface

Rachel Weirnick[1], Andrew R Gosselin[1], Elizabeth Hoyt[1], Effie Ao[1], Prashant K Purohit[2], Valerie Tutwiler[1]

[1]Department of Biomedical Engineering, Rutgers University, New Brunswick, NJ, USA, [2]Department of Mechanical Engineering and Applied Mechanics, University of Pennsylvania, Philadelphia, PA, USA.

Introduction: Thromboembolization presents a significant morbidity and mortality burden when emboli occlude smaller vessels such as in pulmonary embolism and ischemic stroke. Embolization occurs due to the mechanical failure of clots; however, this clinical problem remains understudied from a mechanical standpoint. Embolization can occur as cohesive fracture, meaning within the bulk material of the clot, or adhesive failure, occurring at the interface between the clot and the blood vessel wall. While both failure modes are clinically plausible, the adhesive mode is comparatively unexplored. Both clot and vessel wall composition may vary across individuals and disease states, yet how these variations affect adhesion at the clot-vessel interface is not well understood. Here, we present an *in vitro* peel test platform that allows isolated manipulation of the composition and microstructure of either the blood clot or the vessel wall mimic, allowing us to probe how changes to either side of the interface regulate failure.

Methods: We developed an experimental platform to measure adhesive toughness (GCadhesive) (adhesive energy per unit area) between a vessel wall mimic and a blood clot, using peel testing approaches adapted from the field of fracture mechanics. Collagen gels were used as a simplified mimic for the subendothelial layer that is exposed during vessel injury. Collagen solution (2.5 mg/mL) was added to a 20x70 mm sample chamber and allowed to polymerize for 4 hours. Following gelation, we layered clots formed from commercially available pooled plasma (2.9 mg/mL fibrinogen). Clotting was initiated with CaCl2 (25 mM final concentration) and tissue factor (1-75 pM final concentrations) and clots were allowed to form for 1 hour. Samples were loaded onto a mechanical tester and the clot was peeled from the collagen layer at a controlled displacement of 1.8 mm/min while the sample base was moved horizontally to control peel angle. Forces were measured with a multi-axial load cell. GCadhesive, a measure of the energy required to separate the clot and vessel layers per unit area, was calculated from the plateau force and angle during steady peeling, normalized to sample geometry and accounting for elastic deformation of the peeled material.

Results: We first characterized adhesive fracture in samples with varying thickness of the plasma layer (3-6mm) and performed tests where plasma clots were peeled from collagen and vice versa. We did not detect measurable differences in GCadhesive across these conditions (n=8, one-way ANOVA), verifying that we are measuring the properties of the fibrin-collagen interface rather than bulk properties of either material or the testing configuration. We next varied coagulation activation by modifying the concentration of tissue factor and found decreasing [TF] from 75 to 1 pM yielded an increase in peel strength from 1.17 to 1.96 N/m (n=8, p=0.0231, two-sided Welch's t-test). [TF] regulates the microstructure of the fibrin network, with low concentrations resulting in networks with fewer thick fibers. This result demonstrates that our setup is sensitive to changes in the fibrin network architecture.

Conclusions: We have established a reproducible and modular testing setup to probe how different properties of blood clots and blood vessels affect the adhesive strength at the clot-vessel interface. Our GCadhesive values fall into similar ranges of studies that quantified adhesion between a blood clot and aortic tissue, supporting physiological relevance of this system. Notably, our adhesive toughness values are consistently lower than previous estimates of cohesive toughness, confirming that adhesive failure is a clinically plausible mechanism of embolization. Our finding that lower TF concentrations yield higher adhesive strength suggests that coagulation kinetics, and the resulting fibrin network architecture, directly influence how strongly a clot remains anchored to the vessel wall, which has potential implications for understanding embolization risk in settings of altered coagulation activation. Future work will vary clot composition, for example by modifying fibrinogen concentration and FXIIIa crosslinking, and the vessel mimic, for example to include extracellular matrix components like vWF as well as endothelial cells, to create a more physiologically relevant model and quantify how these changes regulate the adhesive strength at the clot-vessel interface.

ABSTRACT 18:

Platelets encountering the S. aureus virulence factor α-hemolysin undergo a phenotypic switch to increase their immune capacity

Matthew Cooper and Dr. Lawrence Goldfinger

Thomas Jefferson University

Platelets are responsible for maintaining hemostasis in response to vascular damage, but also have extensive roles in the immune response to bacterial infection. These roles include sequestration and clearance through direct interaction with bacteria, but also indirect responses dependent on the secretion of cationic host defense peptides (CHDPs) and immune-activating cytokines. While canonical platelet activation is critical for some aspects of the immune response, it can be also be hijacked by the invading pathogen to cause the clearance of platelets from circulation and aid in immune evasion. Therefore, release of antimicrobial peptides and immune-activating factors by platelets in the absence of canonical activation may be beneficial for the immune response. High doses of the *Staphylococcus aureus* toxin α-hemolysin (Hla) are known to cause platelet activation, degranulation, and lysis. However, platelets that encounter lower, sub-lytic and sub-activating doses of Hla have the opportunity to respond to the toxin in other ways. In this study we demonstrate a phenotypic switch in platelets, whereby upon encountering sub-lytic and sub-activating concentrations (<500 ng/mL) of Hla, normal platelet response to agonists is abolished and immune-related secretion is increased. We report that, following treatment with Hla at sub-activating concentrations for at least 15 minutes, platelet activation as measured by integrin activation, p-selectin exposure, and ATP release in response to normal platelet agonists is completely abolished. Additionally, we observed that the platelet surface glycoproteins GPVI and GPIbα are shed following treatment with sub-activating concentrations of Hla. These platelets express phosphatidylserine on their surfaces but do not express cleaved caspase-3 or demonstrate physical markers of either apoptosis or necrosis as seen by transmission electron microscopy. However, platelets exposed to low concentrations of Hla have activated translation initiation signaling and form the translation initiation complex, as demonstrated by phospho-immunoblotting and γ-aminophenyl-m^7GT respectively. Separation by SDS-page followed by silver stain of platelet releasates showed increased protein content when stimulated with sub-activating doses of Hla.

Liquid chromatography-mass spectrometry (LC-MS) analysis revealed specific protein enrichment in the Hla-stimulated platelet releaseate relative to unstimulated platelet releasate, including enrichment of proteins related to endocytic and autolysomal mechanisms. Release of IL-18 by Hla-stimulated platelets was identified by LC-MS and was confirmed by immunoblot. Results of this study demonstrate a novel platelet immune response to *S. aureus* wherein platelets primed with low concentrations of bacterial toxin adapt to prevent activation and clearance while increasing their potential to activate a robust immune response. Furthermore, these results point to a dual role for platelets in defense against bacterial infection. High concentrations of bacterial virulence factors trigger irreversible responses such as aggregation and bacterial clearance without engaging alternate secretion mechanisms. Alternatively, sub-activating, sub-lytic concentrations, such as may be diluted in peripheral blood, inhibit canonical platelet activation and trigger release of AMPs via noncanonical secretion that may contribute to the immune response to bacterial infection.

ABSTRACT 19:
Thrombin Generation of Hemophilia B-causing Factor IX Variants with Non-Factor Therapies

Kyumin Lee[1], Sebastian Leyes Porello[1], Shelley Fletcher[2,3] Amy Shapiro[4], Jill Johnsen[2,3], Marianne Kjalke[5], Jacob Lund[5], Benjamin Samelson-Jones[1,6]

[1]The Children's Hospital of Philadelphia, Philadelphia, PA, United States; [2]Bloodworks Northwest, Bleeding Disorders Laboratory, Seattle, WA, United States; [3]University of Washington, Department of Medicine, Seattle, WA, United States; [4]Innovative Hematology, Indianapolis, United States; [5]Novo Nordisk A/S, Bagsvaerd, Denmark; [6]University of Pennsylvania, Perelman School of Medicine, Philadelphia, PA, United States.

Introduction: Non-factor therapies (NFT), including factor (F) VIIIa-mimetic bispecific antibodies and anti-TFPI antibodies, are revolutionizing care for hemophilia (H) A and HB. NFTs offer therapeutically relevant improvements in thrombin generation (TG) and resultant clinically meaningful reductions in bleeding with convenient subcutaneous administration. FVIIIa-mimetics are approved for HA, though we recently demonstrated that FVIIIa-mimetics also enhance the activity of select HB-causing FIX-variants (Lee et al. Blood 2024) that encompasses ≥7% of participants in the My Life Our Future database.

Aims: Compare TG by NFT with common HB-causing missense FIX variants.

Methods: TG of HB-causing FIX-variant purified recombinant protein or HB-patient plasma was determined with therapeutic (or likely therapeutic) concentration of FVIIIa-mimetics (300 nM emicizumab, 34 nM Mim8, 10 nM Inno8) and anti-TFPI antibodies (30 nM concizumab, 113 nM mastacimab-SIA). Separately, to model the effects of fitusiran, FIX-variant protein and recombinant antithrombin (AT) were to FIX/AT doubly immunodepleted plasma and was compared to 300 nM emicizumab and 34 nM Mim8 in 2.5 μM AT. All TG was triggered with tissue factor (TF) or FXIa.

Results: FVIIIa-mimetics, anti-TFPI antibodies, and AT depletion increased thrombin generation of recombinant FIX-L6S, FIX-D47E, FIX-R333Q, and FIX-I397T. When triggered by 1 pM TF, anti-TFPI antibodies restored TG for these FIX-variants, while TG with FVIIIa-mimetics was more variable between FIX-variants though most reached normal levels. However, when triggered by 0.1 pM TF or FXIa, FVIIIa mimetics mostly restored TG for these FIX-variants while TG with anti-TFPI antibodies was generally lower and more variable between FIX-variants. Additionally, when triggered by 0.1 pM TF and 1 pM FXIa, FVIIIa-mimetics increased peak thrombin generation comparable to 15% and 0% normal AT.

For the catalytically inert FIX-S365A, as expected, FVIIIa-mimetics did not improve TG regardless of triggering reagent. In HA plasma triggered with 1 pM TF, TG was generally higher with anti-TFPI antibodies than FVIIIa mimetics; conversely, in HA plasma triggered with 0.1 pM TF or FXIa, TG was substantially higher for FVIIIa-mimetics than anti-TFPI antibodies. Mim8 and concizumab also increased TG four-fold and two-fold respectively in FIX-R333Q patient plasma (0.1 pM TF).

Conclusion: TG for FVIIIa-mimetics, anti-TFPI antibodies, and AT depletion is dependent on the FIX-variant and the triggering conditions. TG with FVIII-mimetics is at least comparable to the TG by anti-TFPI antibodies and AT depletion across triggering conditions for these FIX-variants. This supports the continued repurposing of FVIIIa-mimetics for select HB patients**.**

ABSTRACT 20:
The Role of the Exon 7–Encoded Insert in Syk Interdomain B in Platelet Function

Nahid Ramezanpour, Manal Elzoheiry, Carol A Dangelmaier, Liying Guan, Monica N Wright, Alexander Y Tsygankov, and Satya P Kunapuli.

The Sol Sherry Thrombosis Research Center and the Department of Cardiovascular Diseases, Lewis Katz School of Medicine, Temple University, Philadelphia PA 19140

Running title: Altered signaling in Syk-S platelets

Abstract body

Spleen tyrosine kinase (Syk) is a 72 kDa non-receptor tyrosine kinase that is expressed in many hematopoietic cells and contributes to immune cell signaling. Syk exists in two main isoforms: a long isoform (Syk-L) and a shorter isoform (Syk-S). Syk-S lacks a 23-amino-acid region encoded by exon 7, which contains several regulatory phosphorylation sites, including Y290, S289, and S291. In this study, we focused on how deletion of Syk exon 7, which eliminates Syk-L but preserves Syk-S, affects signaling and function using platelets as an experimental system. To evaluate the function of this region, we generated mice in which exon 7 of Syk was deleted (Syk exon 7 knockout mice) using CRISPR-Cas9 gene editing, thereby eliminating Syk-L. Platelets from homozygous Syk exon 7Δ mice showed no reduction in platelet responses after stimulation with AYPGKF, a PAR4 agonist, or 2-MeSADP, a purinergic agonist, but showed significantly reduced signaling after stimulation with GPVI receptor agonist CRP-A or CLEC-2 receptor agonist, CLEC-2 mAb. In addition to reduced ex vivo platelet responses, Syk exon 7Δ mice showed delayed thrombus formation in the $FeCl_3$ injury model, compared with WT littermates. However, tail bleeding time was not significantly different between Syk exon 7Δ mice and WT mice. Together, these data suggest that the exon 7–encoded region of Syk is required for optimal ITAM-and hemITAM-mediated platelet signaling and thrombus formation, without affecting hemostatic responses.

ABSTRACT 21:
Developing OrionEdit, a Novel CRISPR-RT Genome Editing Technology, for Hemophilia B Gene Therapy

Veronika Poliakova and Victor Shengkan Jin.*

Department of Pharmacology, Rutgers University–Robert Wood Johnson Medical School, Piscataway, NJ 08854.

Hemophilia B is an X-linked recessive bleeding disorder caused by mutations in the *F9* gene, resulting in functional coagulation Factor IX (FIX) deficiency. Current standard-of-care relies on replacement therapy using plasma-derived or recombinant factor IX concentrates. They require lifelong prophylactic infusions without offering a cure, presenting substantial patient burden and high economic costs. Recent gene therapy development led to FDA-approved adeno-associated virus (AAV)-mediated gene addition therapy, Hemgenix, that delivers an exogenous F9 expression cassette. This gene addition strategy has critical inherent shortcomings, including

non-permanence and dilution of AAV transgene over time, inability to re-dose, and liver toxicity. The emerging clinical development of CRISPR-mediated homology directed integration of F9 expression cassette provided by an AAV template offers a promise of permanent cure; however, it may face some similar issues of the episomal AAV strategy, including liver toxicity, inability to re-dose if the first try failed, and potential double-strand break (DSB)-induced genotoxicity.

Directly correcting endogenous *F9* mutations offers a mechanistically superior approach, but standard Prime Editing usually remains restricted to correcting short sequences (20–30 bp), whereas *F9* disease mutations are broadly distributed across the gene. To overcome this, we developed OrionEdit, a novel CRISPR-reverse transcriptase (RT) precision editing platform. OrionEdit utilizes three components: a nickase Cas9 (H840A)-RT fusion protein, an engineered guide RNA (magRNA), and an independent modular RNA template. The magRNA recruits the nCas9-RT and template to the target site, incorporating desired edits via target-primed reverse transcription (TPRT). Uncoupling the RNA template from the guide RNA eliminates the intramolecular interference and spatial constraints common to prime editing guide RNAs (pegRNAs), enabling significantly longer reverse transcription templates (RTTs).

Consequently, a single OrionEdit template can potentially correct broad mutation clusters across an entire *F9* exon. As proof of concept, we achieved high-efficiency editing to correct *F9* T342M and R379Q mutations, and introduce the hyperactive Padua variant (R384L). We estimate that 5 to 7 Orion Editors can cover the full clinical spectrum of Hemophilia B mutations. Aligned with recent FDA guidance on gene therapy for 1-to-*n* mutations, OrionEdit establishes a feasible gene therapy platform for correcting the endogenous F9 mutations for treating hemophilia B.

*Email and Disclosure: victor.jin@rutgers.edu. Rutgers University has licensed the OrionEdit patents to GenOrion Therapeutics (V.S.J is a founder) for commercial development.

ABSTRACT 22:

The Incorporation of Machine Learning Models to Predict Thrombotic and Infectious Complications after Spinal Cord Injury

Hajer Ali, Youssef Mourad, Berk Inan, Maya Mikrut, Valerie Tutwiler, Julie Goswami

Background: Acute traumatic spinal cord injury (SCI) is associated with high rates of venous thromboembolism (VTE), with incidences of up to 20%. Patients with SCI are also at increased risk of infections, including urinary tract infections and pneumonia. Demographic features (age and body mass index

- BMI), injury patterns (injury level, severity, function), and clinical course (need for surgery, immobility) are implicated in development of infectious and thrombotic complications after trauma. Early changes in blood clotting after injury, trauma–induced coagulopathy (TIC), are intricately linked to the immune response. However, little is known about how biomarkers of early TIC may predict downstream complications. In this study, we incorporate clinical features with early biochemical TIC into machine learning (ML) models to predict infectious and thrombotic events (VTE) after SCI.

Methods: This is a single institution retrospective cohort study performed at our Level 1 Trauma Center. After obtaining approval from the institutional review board, we performed chart review of patients presenting as trauma activations who were identified to have suffered SCI. Clinical features and laboratory values were obtained using the institutional Trauma Registry and electronic medical record. Trauma-induced coagulopathy (TIC) was included as a feature in these models as a composite value of INR > 1.2, PT > 18s, or aPTT > 60s. Our primary outcomes were VTE or infectious complications. Statistical analysis was performed with GraphPad Prism. All data expressed as median and quartiles [Q1, Q3].

ML strategies included XGBoost, Logistic Regression, Random Forest Importance, and Support Vector Machine (SVM). The feature importance of the preliminary variables was determined using LASSO Logistic Regression, Recursive Feature Elimination with Cross-Validation (RFECV), and Random Forest Importance.

Results: We identified 136 patients with SCI who presented to our Level 1 trauma center between 2021 and 2025. The median age was 64 [41.0, 73.2] and median injury severity score (ISS) 17.0 [14.0, 26.0]. Of these patients, 70.6% were male, the overwhelming majority (92.6%) suffered blunt mechanisms, and 75.0% had injuries at the cervical spine level. There were 20 (14.7%) mortalities, 20 (14.7%) patients with VTE, and 22 (16.2%) patients with infectious complications. Patients who suffered VTE had comparable age, BMI, ISS, and presenting laboratory values, but were more likely to have undergone surgery as compared to those without VTE. Patients who suffered infectious complications had comparable demographics, slightly increased admission INR, and comparable rates of surgery as compared to those without infectious complications.

Of the ML models tested, SVM performed the best at predicting VTE, while logistic regression outperformed for infectious complications. The top five predictors of VTE were INR, injury at the

lower cervical level, presenting heart rate, hemoglobin, and ASIA Impairment Scale. Meanwhile, the top five predictors of infectious complications were the presence of TIC, heart rate, ISS, aPTT, and Age. Across 5-fold cross-validated sets, the SVM model produced a mean Area Under the Curve (AUC) of 0.813 ± 0.08 for VTE predictions, and logistic regression computed a mean AUC of 0.748 ± 0.015 for sepsis.

Conclusion: While there is limited statistically significant differentiation for SCI patients who develop VTE or infectious complications by conventional analysis, ML modeling is able to identify composite features that may allow for early identification of those most at risk in these vulnerable populations. Furthermore, TIC is the top predictor of infectious complications, supporting the intricate link between coagulation and immune processes in response to traumatic injury.

ABSTRACT 23:

Modulation of BAK1 Expression by Megakaryocyte/Platelet-Targeted siRNA Reduces Apoptotic Changes and Promotes Platelet Survival

Amir Yarahmadi, PhD; Shayan Askari, PhD; Jeremy Wurtzel, MS; Lawrence Goldfinger, PhD

Cardeza Foundation for Hematologic Research, Division of Hematology, Department of Medicine, Sidney Kimmel Medical College, Thomas Jefferson University, Philadelphia, PA, USA

Background: Platelet transfusion is an essential therapy for the prevention and treatment of bleeding disorders; however, its effectiveness is limited by platelet storage lesion (PSL), a progressive deterioration that occurs during storage and compromises post-transfusion platelet recovery and survival. Apoptosis is a key contributor to PSL and is characterized by mitochondrial dysfunction, phosphatidylserine (PS) exposure, platelet activation, and accelerated clearance. The pro-apoptotic protein BCL-2 homologous antagonist/killer 1 (BAK1) is a critical regulator of intrinsic apoptosis and platelet lifespan. We hypothesized that selective suppression of BAK1 expression could reduce platelet apoptosis during storage and improve post-transfusion platelet recovery and survival.

Aim: To evaluate whether megakaryocyte-/platelet-selective modified siRNA (stimRNA) targeting BAK1 can suppress intrinsic apoptotic signaling, preserve platelet quality during storage, and enhance platelet survival following transfusion.

Methods: We used a formulated siRNA (stimRNA) containing stability-enhancing nucleotide modifications that selectively target megakaryocytes and platelets following *in vivo* or *ex vivo* administration. BAK1 stimRNA was incubated *ex vivo* with human platelet-rich plasma stored at room temperature for up to 5 days or administered naked in saline solution to mice for *in vivo* studies. Expression of BAK1 and other apoptosis-related proteins Bax, cleaved caspase-3, and Bcl-xL were assessed by immunoblotting. Platelet apoptotic and activation markers, including PS exposure, PAC-1 binding, and P-selectin expression were quantified by flow cytometry. Mitochondrial membrane potential (Δψm) was assessed using tetramethyl rhodamine ethyl ester (TMRE) staining. Platelet function was determined by light transmission aggregometry. *In vivo* platelet lifespan and transfusion outcomes were evaluated using fluorescently labeled murine platelets and by transfusion of human platelets into immunodeficient NSG mice.

Results: Treatment with BAK1-targeting stimRNA achieved effective knockdown of BAK1 protein expression in both murine and human platelets. In stored human platelets, BAK1 expression increased progressively during storage, whereas BAK1 stimRNA treatment prevented this increase and maintained BAK1 expression near baseline levels. BAK1 silencing was associated with attenuation of intrinsic apoptotic signaling, evidenced by reduced cleaved caspase-3 expression, decreased PS exposure, and improved preservation of mitochondrial membrane potential (Δψm). During storage, PS and P-selectin expression increased markedly after 72 and 96 hours; however, BAK1 stimRNA significantly mitigated PS exposure at 72 hours, indicating reduced platelet apoptosis. Aggregation responses and platelet activation markers, including PAC-1 binding following agonist stimulation were largely preserved, demonstrating maintenance of platelet hemostatic capacity. In mice, *in vivo* fluorescent platelet tracking demonstrated that platelets form BAK1 stimRNA treated mice exhibited reduced apoptotic signaling, preserved mitochondrial membrane potential and prolonged circulation compared with control platelets. Most importantly, BAK1-targeted stimRNA significantly improved human platelet recovery and survival following transfusion into immunodeficient NSG mice.

Conclusions: Selective suppression of BAK1 using platelet-targeted stimRNA reduces intrinsic apoptotic signaling, preserves mitochondrial integrity, and mitigates features of platelet storage lesion without compromising platelet function. BAK1 silencing significantly improves post-transfusion recovery and survival *in vivo*, supporting BAK1 as a promising therapeutic target for extending platelet shelf life and enhancing transfusion efficacy. These findings establish platelet-directed RNA therapeutics as a novel strategy to improve platelet storage quality and transfusion outcomes.

ABSTRACT 24:

Platelet FcγRIIA drives thrombo-inflammatory reperfusion injury following ischemic stroke through PLCγ2-dependent and PLCγ2-independent mechanisms

Jared C Whitman, and Lawrence E Goldfinger

Background: Although thrombectomy and thrombolysis restore cerebral blood flow after ischemic stroke, reperfusion can trigger secondary injury through poorly understood mechanisms involving thrombo-inflammation. Platelets are increasingly recognized as central mediators of post-ischemic

inflammation and vascular dysfunction in addition to thrombosis. Platelet immunoreceptor tyrosine-based activation motif (ITAM) signaling, including the downstream effector phospholipase Cγ2 (PLCγ2), regulates platelet activation and thrombo-inflammatory responses. FcγRIIA, a human-specific low-affinity IgG receptor on platelets, promotes platelet activation through ITAM-associated signaling. Clinical studies associate elevated platelet FcγRIIA expression with worse neurological outcomes following stroke; however, its contribution to cerebral reperfusion injury and the role of downstream PLCγ2 signaling remain undefined. We hypothesized that platelet FcγRIIA contributes to thrombo-inflammatory cerebral reperfusion injury through both PLCγ2-dependent and PLCγ2-independent signaling, with FcγRIIA suppression providing greater protection than PLCγ2 suppression alone.

Methods: We employed SiRNA harboring modified nucleotides (“StimRNAs”), which we have found are stable in circulation, and selectively target megakaryocytes and platelets upon administration in saline suspension in vivo. Humanized FCGR2A transgenic mice, which express human FcγRIIA on platelets, were treated with StimRNAs targeting FcγRIIA, PLCγ2, or both. Flow cytometry quantified platelet FcγRIIA surface expression and reactivity following FcγRIIA-, GPVI-, and protease-activated receptor (PAR)-specific agonists by measuring α-granule release and αIIbβ3 integrin activation. PLCγ2 expression was assessed by immunoblotting. Transient middle cerebral artery occlusion (tMCAO) was performed 48 hours after StimRNA administration, and infarct volume was quantified by ImageJ 24 hours after reperfusion.

Results: FcγRIIA-specific StimRNA significantly reduced platelet FcγRIIA surface expression at 24 and 48 hours, while PLCγ2-specific StimRNA similarly reduced PLCγ2 protein expression. FcγRIIA suppression reduced platelet P-selectin exposure and αIIbβ3 integrin activation following FcγRIIA-mediated activation, while GPVI- and PAR-specific signaling were preserved. Selective PLCγ2 suppression reduced P-selectin exposure and αIIbβ3 integrin activation following both GPVI- and FcγRIIA-mediated activation, while PAR signaling remained unaffected. Following tMCAO, FcγRIIA suppression produced a 50.57 ± 6.8% reduction in infarct volume compared with control StimRNA-treated mice, establishing a functional contribution of platelet FcγRIIA to post-ischemic cerebral injury. Targeting PLCγ2 alone produced a 24.5 ± 7.42% reduction in infarct volume compared with controls, supporting a role for PLCγ2 in reperfusion injury. Notably, simultaneous targeting of FcγRIIA and PLCγ2 produced the greatest protection, resulting in a 60.24 ± 7.7% reduction in infarct volume compared with controls and a 47.34 ± 10.2% additional reduction compared with PLCγ2 suppression alone. Together, these findings indicate that suppression of the shared downstream ITAM effector PLCγ2 does not fully recapitulate the protective effect of reducing platelet FcγRIIA expression, suggesting that FcγRIIA contributes to ischemic injury through both PLCγ2-dependent and PLCγ2-independent mechanisms.

Conclusion: These findings identify platelet FcγRIIA surface expression as an important regulator of thrombo-inflammatory reperfusion injury following ischemic stroke. The differential effects of FcγRIIA and PLCγ2 suppression demonstrate that FcγRIIA-mediated injury cannot be explained solely by canonical PLCγ2-dependent ITAM signaling, and support complementary PLCγ2-dependent and PLCγ2-independent mechanisms. The involvement of PLCγ2 in GPVI-mediated platelet responses suggests pathway-specific functions during reperfusion, potentially contributing to pathogenic platelet activation and vascular protective responses. Defining these pathways may provide a framework for selectively targeting detrimental FcγRIIA-mediated platelet activation while preserving beneficial platelet signaling required for vascular integrity. Together, these findings identify platelet FcγRIIA and PLCγ2 as critical regulators of thrombo-inflammatory reperfusion injury, with FcγRIIA contributing to injury through both PLCγ2-dependent and PLCγ2-independent mechanisms.

ABSTRACT 25:

Platelet Microarchitecture Regulates Coagulation Factor Transport and Reaction Rates in Three-Dimensional Reconstructions of Hemostatic Thrombi

Catherine House[1], Scott L. Diamond[1], Maurizio Tomaiuolo[2], Timothy J. Stalker[3], and Talid Sinno[1]

[1] Department of Chemical and Biomolecular Engineering, University of Pennsylvania, Philadelphia, Pennsylvania, United States of America; [2]Cardeza Foundation for Hematological Research, Department of Medicine, Thomas Jefferson University, Philadelphia, Pennsylvania, United States of America; [3]Department of Pediatrics, Children's Hospital of Philadelphia, Philadelphia, Pennsylvania, United States of America

Abstract: When formed in vivo, hemostatic thrombi exhibit a heterogeneous architecture comprised of distinct regions of densely and sparsely packed platelets. This architecture creates a complex interplatelet pore network through which plasma-borne coagulation proteins and agonists move and react, with reactions occurring either within the pore space or at activated platelet surfaces. Thrombus microarchitecture thus serves as both a scaffold and a fetter for coagulation, providing reactive surfaces while restricting molecular transport. This relationship between architecture, transport, and reaction, which plays out on the scale of nanometers and microseconds, is difficult to experimentally characterize and remains poorly understood. To investigate how platelet microarchitecture influences molecular transport and reaction rates we developed a computational pipeline combining high-resolution electron microscopy, machine-learning-based segmentation, and physics-driven simulations. Serial Block Face – Scanning Electron Microscopy was used to image select volumes of hemostatic masses formed in a mouse jugular vein, producing large stacks of 2D images. The images in each stack were segmented using machine learning software and connected to create 3D reconstructions of clot microarchitecture. These reconstructions were utilized as computational domains for Lattice Kinetic Monte-Carlo (LKMC) simulations, allowing molecular transport and reaction to be modeled within real clot geometries. This study features two such reconstructions: one 14 × 14× 10 μm dense core region (pore fraction = 0.07) and one 14 × 14 × 4 μm sparse shell region (pore fraction = 0.32). We simulated the diffusion of 5 nm-diameter molecules in each domain at a free rate of *Dfree* = 100 $\mu m^2/s$ (comparable to thrombin in body-temperature plasma). It was found that effective molecular diffusion rate *Deff* evolves with exploration length *l*. At short exploration lengths there are few interactions with surfaces and *Deff* is close to the free rate *Dfree*. However with increasing *l* and repeated surface encounters, transport rates are progressively reduced, reaching asymptotic *Deff* values of 0.45**Dfree* in the sparse shell and 0.03* *Dfree* in the dense core. Likewise, variability in transport rates between individual molecules is greatest at short exploration lengths but decreases as molecules sample further architecture and foster a more homogenous experience of the domain. These findings indicate that the impact of clot architecture on molecular transport depends strongly on the spatial and temporal scale over which a molecule explores the thrombus. This scale dependence is foundational to understanding how clot structures influence reaction rates. For reactions involving high reagent concentrations and low activation energies, such as the conversion of fibrinogen to fibrin by thrombin, reaction occurs on a scale over which reagent trajectories are not meaningfully constrained by local architecture. Reaction rates under these conditions are not sensitive to thrombus architecture. In contrast, reactions involving low reagent concentrations and/or high activation energies, such as the inhibition of thrombin by antithrombin-III, occur at a length scale wherein reagents have an extensive and homogeneous experience of the domain; these reaction rates are greatly influenced by thrombus architecture. LKMC simulations of bimolecular reactions within the reconstructed domains supported this indicated relationship between architecture, reactant concentration, reaction kinetics, and effective reaction rate. These results ultimately suggest that platelet architecture selectively regulates different coagulation reactions according to the characteristic lifetime and mobility of their reactants. This behavior is emergent from our imaging-to-simulation framework and is opaque to continuum models. The reactions of the coagulation cascade span a range of activation energies, and involve reagents at continually fluctuating concentrations ranging from 50-5000 nanomoles per liter. Capturing how these reactions are modulated by thrombus structure requires linking detailed platelet architecture to molecular transport and reaction. Only by making this connection can we determine how local platelet architecture shapes the dynamics of coagulation.

ABSTRACT 26:

Platelet-selective naked modified siRNA suppression of prostacyclin pathway mediators improves hemostasis in mice

Harriet Ghansah, Jeremy Wurtzel, Timothy Stalker, Lawrence Goldfinger

Cardeza Foundation for Hematologic Research, Thomas Jefferson University, Philadelphia, PA, United States

Background: Platelet activation is regulated by a balance between stimulatory and inhibitory signaling pathways. Gαs (gene, Gnas) and the IP receptor (gene, Ptgir) are key components of the latter pathway. Prostacyclin (PGI2) inhibits platelet function by binding to the IP receptor on the platelet surface, activating the Gαs protein. Gαs subsequently stimulates adenylyl cyclase, leading to an increase in intracellular cyclic adenosine monophosphate (cAMP), and thereby counteracting ADP/P2Y12 Gi-mediated activation pathways.

Hypothesis: We hypothesized that platelet-targeted modulation of Ptgir and Gnas may serve as a possible approach to improve hemostasis in murine models of acquired bleeding without increasing thrombotic risk.

Methods: To test this hypothesis, we designed a novel short tissue-targeted inhibitory modified RNA (stimRNA) targeting Gnas or Ptgir. We have found that siRNAs harboring modified nucleotides (stimRNAs) are stable in circulation and selectively transfect megakaryocytes and platelets *in vivo*. Naked Gnas or Ptgir stimRNAs were administered intravenously to wild-type (WT) and Hermansky–Pudlak syndrome (HPS) mice (dense granule deficiency) for 24 h. Protein expression levels in WT mice were quantified by immunoblotting. PGI2-mediated signaling was evaluated by measuring intracellular cAMP levels, phosphorylation of vasodilator-stimulated phosphoprotein (p-VASP), Jon/A binding, and platelet aggregation with adenosine diphosphate (ADP) in the presence of PGI2 at assay-specific concentrations ranging from 10 to 100 nM. Platelet hemostatic function was assessed using tail bleeding and jugular vein puncture models.

Results: In WT mice, western blot analysis showed 32% and 31% reductions in Gnas and Ptgir protein expression, respectively, following treatment with 0.5 mg/kg of stimRNA. cAMP levels were reduced in mice treated with 0.5 mg/kg of Gnas or Ptgir stimRNA compared with saline-treated controls. Consistent with attenuation of inhibitory signaling, p-VASP was reduced, and Jon/A binding (αIIbβ3 activation) and platelet aggregation with ADP in the presence of PGI2 were increased in stimRNA-treated mice compared to controls. In contrast, thrombin-induced Jon/A binding was comparable between treated and control mice, indicating that Gnas and Ptgir suppression preferentially modulates PGI2-mediated platelet inhibition. Functionally, Gnas or Ptgir knockdown reduced blood loss and shortened bleeding times in both tail bleeding and jugular vein puncture models. Notably, treatment with Gnas or Ptgir stimRNA also reversed bleeding induced by either a low (0.5 mg/kg) or high dose (10 mg/kg) of ticagrelor, a P2Y12 receptor antagonist. In ferric chloride-induced thrombosis models, we observed increased thrombus formation in ticagrelor-treated mice that received Ptgir stimRNA, suggesting a dominant role for Ptgir in this pathway. In HPS mice, Ptgir stimRNA treatment failed to correct the bleeding phenotype despite increased platelet accumulation, suggesting that its pro-hemostatic effect may be insufficient to overcome the substantial bleeding defect in the absence of dense granules.

Conclusions: Platelet-targeted stimRNAs accelerate hemostasis *in vivo* and are effective in reversing acquired but not inherited bleeding in these models. These findings underscore important roles for P2Y12/Gi-independent roles for adenosine triphosphate (ATP) and ADP in bleeding associated with dense granule deficiency.

ABSTRACT 27:
Acidosis and Hypothermia Synergistically Delay Clotting and Reduce Fibrinolysis

Urooj Saeed[1], Andrew R. Gosselin[1], and Valerie Tutwiler[1]

[1] Rutgers University, Department of Biomedical Engineering, New Brunswick, NJ, USA

Background: Traumatic injury is a leading cause of death worldwide, with hemorrhage accounting for approximately 40% of trauma-related fatalities. Hypothermia and acidosis commonly develop following severe trauma and are associated with impaired coagulation, increased bleeding risk, and poor outcomes. Despite their clinical significance, their individual and combined effects on clot formation and stability remain incompletely understood. This study investigates how hypothermia and acidosis alter fibrin clot formation, mechanics, structure, and fibrinolysis.

Methods: Pooled human platelet-poor plasma (PPP) with a starting fibrinogen concentration of 2.5 mg/mL was evaluated under hypothermic conditions ranging from 37–22°C, acidotic conditions ranging from pH 7.80–7.00, and fibrinogen concentrations ranging from 2.5–1 mg/mL. Acidosis was induced with HCl supplementation, dilutions were induced with sodium chloride and samples were activated with 1 pM tissue factor and 25mM $CaCl_2$. Fibrinolysis was induced with 225 ng/mL tissue plasminogen activator (tPA) when indicated. Acidosis and hypothermia were also assessed under simulated trauma conditions using a simulated trauma-induced coagulopathy (STIC) model where coagulation kinetics observed in trauma patients was recreated by diluting platelet poor plasma (2.5 mg/mL fibrinogen) with a 15% volume dilution of normal saline, activated with 45 pM tissue factor (TF) and 225 ng/mL tPA. Clot formation and fibrinolysis were assessed for 1 hour using an Anton Paar MCR302e temperature-controlled rheometer to quantify clot viscoelasticity and stiffness and a temperature controlled Molecular Devices SpectraMax Plus plate reader to assess fibrin polymerization and lysis kinetics through optical turbidity. Outcomes included lag time, clotting rate, maximum clot formation and stiffness, and fibrinolysis rate. Fibrin network structure was assessed using a Zeiss LSM 710 confocal microscope (Zeiss, Oberkochen, Germany) with 1% of the total plasma volume substituted with 1.5 mg/mL Alexa Fluor 488–conjugated fibrinogen (Thermo Fisher Scientific, USA) for fluorescent visualization. Statistical analyses included one- and two-way ANOVA and Spearman correlations, with data reported as mean ± SEM.

Results: Decreasing fibrinogen concentration reduced maximum clot stiffness and optical density, with rheology demonstrating a reduced clotting rate at the lowest fibrinogen concentration, while turbidity showed increased clotting rate with dilution. Hypothermia prolonged clotting lag time and reduced clotting rate without significantly altering final clot stiffness or optical density, whereas acidosis alone at 37°C did not significantly affect clotting kinetics or final clot properties. Hypothermia and reduced fibrinogen concentration did not significantly alter fibrin network density, while basic pH increased fibrin fiber density and severe acidosis had no significant effect. Fibrinogen concentration remained the primary driver of plasma clot formation when reduced fibrinogen and acidosis were combined, with minimal additional effects from acidosis. Similarly, clot formation impairment under combined hypothermic and acidotic conditions was primarily driven by hypothermia. In fibrinolytic conditions, hypothermia and severe acidosis independently reduced fibrinolytic rate, with combined severe acidosis and hypothermia producing the greatest reduction in fibrinolytic rate. In the STIC model, hypothermia delayed clot formation and reduced fibrinolysis, while acidosis primarily reduced fibrinolysis; combined hypothermia and acidosis further reduced fibrinolysis compared with either condition alone.

Conclusion: Hypothermia and acidosis exert distinct yet cooperative effects on coagulation and fibrinolysis. Hypothermia primarily delays clot formation and reduces fibrinolysis, while acidosis has limited effects on clot formation but independently impairs fibrinolysis. Together, hypothermia and acidosis further reduce fibrinolytic activity and prolong clot persistence. These findings provide mechanistic insight into trauma-associated coagulation dysfunction and highlight the importance of maintaining physiological temperature and pH during trauma resuscitation.

ABSTRACT 28:

Factor H Host-Recognition Domains Confer Tissue-Specific Protection in Renal and Extrarenal Vascular Beds

Jing Hu, Takashi Miwa, Eshagh Mohammadyari, Madhu Golla, Lakshmi Pravallika Poka, William Halle, Lin Zhou, and Wen-Chao Song

Department of Systems Pharmacology and Translational Therapeutics, Perelman School of Medicine, University of Pennsylvania, Philadelphia, PA 19104

Background: Factor H (FH) is the principal regulator of alternative pathway (AP) complement activation, and FH mutations are associated with atypical hemolytic uremic syndrome (aHUS). Gangrene, characterized by ischemia and necrosis of distal extremities, occurs in a subset of aHUS patients, but a direct link between FH dysfunction and gangrene has not been established. Here, we describe a mouse model of complement-mediated gangrene resulting from FH dysfunction.

Methods: We studied an FH hypomorphic mutant mouse ($FH^{m/m}$) expressing trace amounts of FH SCR1-18, resulting in plasma C3 and factor B (FB) consumption, prominent glomerular C3 deposition, and mild C3 glomerulopathy. Mice were treated with adeno-associated virus 8 (AAV8) vectors encoding IgG1-Fc fusion proteins containing FH SCR1-4 alone, FH SCR1-4/6-8, or FH SCR1-4/6-8/19-20. These constructs retain fluid-phase AP regulatory activity but differ in host cell-binding domains. Mice were followed for 6 weeks.

Results: All FH fusion proteins were persistently expressed in plasma and restored C3 and FB levels. FH SCR1-4-Fc achieved the highest circulating concentration, likely due to the absence of host cell-binding domains, and completely normalized plasma C3 and FB, whereas FH SCR1-4/6-8-Fc and FH SCR1-4/6-8/19-20-Fc produced only partial recovery. Unexpectedly, mice treated with FH SCR1-4/6-8-Fc developed severe tail necrosis, gangrene, and stroke-related mortality, whereas those receiving FH SCR1-4-Fc or FH SCR1-4/6-8/19-20-Fc did not. FH SCR1-4/6-8-Fc partially, and FH SCR1-4/6-8/19-20-Fc completely, prevented glomerular C3 deposition.

Conclusions: These findings establish a mouse model of complement-mediated gangrene and suggest that distinct FH host-recognition domains confer tissue-specific protection in renal and extrarenal vascular beds.

ABSTRACT 29:

Structural basis for the intrinsic Xase assembly on a procoagulant membrane and the development of factor VIIIa-mediated activity, revealed by cryo-electron microscopy

Vladimir Kolyadko, Ruth Pumroy, Vera Moiseenkova-Bell, Sriram Krishnaswamy

Research Institute, Children's Hospital of Philadelphia, Philadelphia, PA

Abstract

Coagulation factor VIIIa (FVIIIa) is a cofactor protein that sequesters the proteinase, factor IXa (FIXa), on the membrane surface of procoagulant platelets to form the membrane-assembled intrinsic Xase complex. The intrinsic Xase is a crucial component of the coagulation system that regulates the hemostatic response, as deficiencies in its components cause hemophilia A and B. The emerging evidence on prothrombotic mutations in FVIIIa and FIXa, such as FVIII-Aurora (R571S mutation in the FVIII-A2 domain) and FIX-Padua (R170L mutation in the FIX catalytic domain), suggests an important role of the intrinsic Xase in the development of thrombosis. The molecular mechanism driving the assembly and function of the FVIIIa-FIXa-membrane complex remains elusive, as numerous conflicting models were previously proposed while experimental studies failed to provide high-resolution structural information. Here, we report a high-resolution cryo-electron microscopy (Cryo-EM) structure of the FVIIIa-FIXa (intrinsic Xase) complex on a procoagulant membrane. The intrinsic Xase was assembled with purified human full-length FVIII and FIXa (S195A), and small unilamellar vesicles containing 25% phosphatidylserine (Ptd-Ser), followed by treatment with thrombin before vitrification of the specimen on Cryo-EM grids. Analysis by SDS-PAGE confirmed quantitative conversion of FVIII into FVIIIa. The FVIIIa-FIXa structure, determined at 2.8-angstrom resolution, reveals the molecular architecture of thrombin-activated FVIIIa and identifies an extended interaction interface with FIXa. Comparison of the FVIIIa-FIXa structure with the 2.6-angstrom structure of the FVIII-FIXa complex provides new insights into the mechanistic basis of cofactor activity upon thrombin-catalyzed activation. Strikingly, the proteinase domain of FIXa is well resolved due to its stabilization in the complex with FVIIIa, while the FIXa proteinase domain in the complex with FVIII (without activation by thrombin) is motile and unable to form stable interactions. This difference is attributed to the stabilization of the acidic regions a1 and a3 in thrombin-activated FVIIIa, which engage an exosite in the FIXa proteinase domain and lock the loop in FVIIIa cleaved by activated protein C (aPC). These changes suggest potential mechanisms for allosteric regulation of FIXa and the protection of FVIIIa from degradation by aPC. Interestingly, the structure of the intrinsic Xase reveals that the FVIIIa Arg571 residue (the site of the prothrombotic FVIII-Aurora mutation) and the FIXa Arg170 residue (the site of the prothrombotic FIX-Padua mutation) belong to the same structural motif stabilized between FVIIIa and FIXa. This highlights the importance of the interactions revealed in the FVIIIa-FIXa complex in hemostasis and thrombosis. Finally, the structure of the intrinsic Xase further suggests a putative binding site for docking the substrate, factor X. In summary, our work provides atomistic details of the intrinsic Xase function, enabled by the high-resolution Cryo-EM structures. These structures bridge the existing functional data with the structural biology of FVIIIa and FIXa, allowing insights into the nature of cofactor activity and its role in regulating the Xase function.

ABSTRACT 30:

Genetic Evidence for Classical Pathway Involvement in Factor H Mutation-Associated Complement-Mediated Thrombotic Microangiopathy

Madhu Golla[1], Damodar Gullipalli[1], Sayaka Sato[1], Miwa Takashi[1], Matthew Palmer[2] and Wen-Chao Song[1*].

[1]Department of Systems Pharmacology and Translational Therapeutics, Perelman School of Medicine, University of Pennsylvania, Philadelphia, PA 19104, [2]Department of Pathology and Laboratory Medicine, Perelman School of Medicine, University of Pennsylvania, Philadelphia, PA.

Background. Atypical hemolytic uremic syndrome (aHUS) is a complement-mediated

thrombotic microangiopathy (TMA) that can be treated with the anti-C5 monoclonal antibody eculizumab. Although alternative pathway (AP) dysregulation is central to disease pathogenesis, the contributions of the classical and lectin pathways to complement-mediated TMA (CM-TMA) has not been rigorously investigated experimentally.

Methods. Mannan-binding lectin serine protease 2 deficient ($Masp2^{-/-}$), Complement component 4 knockout ($C4^{-/-}$), and Complement protein C1q knockout ($C1q^{-/-}$) mice were crossed with Factor H ($FH^{R/R}$) mice harboring a homozygous W1206R mutation in factor H, a murine model of CM-TMA. Survival, hematologic parameters, renal function, thrombotic pathology, and clinical manifestations were assessed.

Results. $FH^{R/R}$ mice exhibited ~41% mortality by 15 weeks of age and developed renal TMA,

glomerular microthrombi, large-vein thrombosis, and neurological abnormalities. In contrast, all $C4^{-/-}/FH^{R/R}$ mice survived, and C1q deficiency conferred similar protection. MASP-2 deficiency did not improve survival, with $Masp2^{-/-}/ FH^{R/R}$ mice exhibiting disease comparable to $FH^{R/R}$ mice. Platelet counts, hemoglobin levels, and reticulocyte counts were similar among groups. However, blood urea nitrogen levels were significantly reduced in $C4^{-/-}/FH^{R/R}$ and $C1q^{-/-}/FH^{R/R}$ mice, indicating protection from renal injury. Histologic analysis demonstrated marked reductions in mesangial matrix expansion, endothelial swelling, glomerular microthrombi, and large-vein thrombosis in $C4^{-/-}/FH^{R/R}$ and $C1q^{-/-}/FH^{R/R}$ mice, but not in $Masp2^{-/-}/ FH^{R/R}$ mice.

Conclusions. These findings identify a critical role for the classical pathway in FH mutation-associated CM-TMA and demonstrate that MASP-2 and the lectin pathway are dispensable for disease development. These results do not support a pathogenic role for MASP-2 in this genetically model of complement-mediated TMA, despite the use of MASP-2 inhibition in hematopoietic stem cell transplant-associated TMA.

ABSTRACT 31:
Complement regulatory context determines the renal phenotype of anti-factor H autoantibodies

Eshagh Mohammadyari, Takashi Miwa, Madhu Golla, Jing Hu, Lin Zhou, William Halle, Matthew Palmer, and Wen-Chao Song

Perelman School of Medicine, University of Pennsylvania, Philadelphia, Pennsylvania

Background: Anti-factor H (FH) autoantibodies are associated with both atypical hemolytic uremic syndrome (aHUS) and C3 glomerulopathy (C3G), but how similar autoantibodies produce these distinct kidney phenotypes remains unclear.

Methods: We used adeno-associated virus serotype 8 (AAV8)-mediated gene delivery to induce chronic expression of mAb 7-1, an anti-mouse FH IgG1 that binds short consensus repeat 20 and impairs FH regulation on host surfaces. Wild-type and genetically modified mice were assessed for renal function, urine abnormalities, complement consumption, renal histopathology, and glomerular complement deposition. Complement- and Fc receptor-deficient mice and an Fc-mutant antibody were used to define disease mechanisms.

Results: AAV8-mAb 7-1 produced persistent, high-level antibody expression in wild-type mice and caused severe C3G-like renal injury, with increased blood urea nitrogen, proteinuria, and hematuria. Histologic findings included glomerular hypercellularity, inflammatory cell infiltration, crescent formation, and tubular injury. Immunofluorescence showed prominent glomerular C3 and C9 deposition with minimal IgG. Plasma C3 and factor B were reduced, consistent with alternative pathway activation and consumption, whereas plasma FH was increased. Loss of C3, factor B, properdin, C5a receptor 1, or the common Fc receptor gamma chain was protective, whereas loss of C4 or C6 was not fully protective. These findings establish essential roles for the alternative pathway, C5a receptor 1, and activating Fc receptors, without an absolute requirement for the classical pathway or membrane attack complex. In decay-accelerating factor-deficient mice, the same antibody caused earlier and more severe renal injury with endothelial swelling and other thrombotic microangiopathy-like features.

Conclusions: A single C-terminal anti-FH autoantibody can produce distinct C3G-like or thrombotic microangiopathy-like kidney injury depending on the host complement regulatory context. Alternative pathway amplification, C5a receptor 1 signaling, and Fc receptor engagement are convergent drivers of anti-FH autoantibody-mediated renal disease.

ABSTRACT 32:

Engineering a Multifunctional Factor V to Effectively Support Both Intrinsic Tenase and Prothrombinase Functions

Shekhar Kumar, PhD[1,2] and Sriram Krishnaswamy, PhD[1,2]

[1]Research Institute, Children's Hospital of Philadelphia, Philadelphia, PA; [2]Pediatrics, University of Pennsylvania, Philadelphia, PA

Factor VIIIa (FVIIIa) promotes intrinsic tenase assembly by localizing factor IXa (FIXa) and factor X (FX) to anionic phospholipid membranes, whereas factor Va (FVa) supports downstream prothrombinase activity. FVIII-mimetic antibodies such as emicizumab approximate FIXa and FX but lack the high-affinity membrane interaction characteristic of FVIIIa. This distinction likely contributes to the ability of FVIIIa to function at sub-nanomolar concentrations and markedly accelerate FX activation, whereas substantially higher concentrations of emicizumab produce more modest rate enhancement. We previously showed that tethering an emicizumab-derived monospecific FIXa-binding scFv to membrane-binding C2 domains derived from either FV or lactadherin substantially enhances FVIII-mimetic activity, despite the relatively modest membrane binding affinity conferred by the isolated C2 domains. Here, we evaluate an alternative design that incorporates the FIXa-binding scFv into a B-domain-deleted FV variant. This architecture intends to further strengthen membrane anchoring of FIXa by exploiting the high-affinity membrane binding properties of the FV C1/C2 domains together. Additionally, this scaffold may also facilitate the intramolecular channeling of nascent FXa directly to the FVa moiety without diffusion constraints, potentially enabling tenase and prothrombinase like functions within a single molecule.

To test this concept, an scFv derived from the FIXa-binding arm of emicizumab was fused to the C-terminus of FV Short, a naturally occurring FV variant with a truncated B-domain, to generate OctaV. Functional activity was evaluated using clotting and thrombin-generation assays in FVIII-deficient, FV-deficient, and combined FV/FVIII-deficient plasma models. OctaV retained the high-affinity phospholipid binding characteristic of FV (apparent Kd ≈2.4 nM), while the fused scFv retained FIXa-binding affinity. Together, these properties enabled membrane localization of FIXa while preserving the prothrombinase cofactor function of the FV scaffold. OctaV corrected clotting defects in FV- and FVIII-deficient plasma and retained potent activity in FV-deficient plasma containing FVIII inhibitory antibodies, effectively modeling combined FV/FVIII deficiency. In FVIII-deficient plasma triggered with 0.1 pM tissue factor and 4 μM PCPS, OctaV produced robust thrombin generation and required nearly 16-fold lower concentrations than emicizumab to achieve comparable peak thrombin. Robust thrombin generation was similarly observed in FV-deficient and combined FV/FVIII-deficient plasmas, further demonstrating the dual cofactor activity of OctaV. The importance of membrane localization was demonstrated using the FV C2 domain-binding E9 scFv. Blocking FV C2-mediated membrane binding effectively suppressed OctaV-driven thrombin generation, demonstrating that membrane localization is a major determinant of its cofactor activity while also providing a potential mechanism for targeted reversal. Engineering activated protein C (APC) resistance in OctaV further enhanced the robustness of the platform under thrombomodulin-mediated anticoagulant pressure. In FVIII-deficient plasma containing 10 nM soluble thrombomodulin, the APC resistant variant showed substantially greater molar potency than emicizumab, with approximately 15 nM APC resistant OctaV generating peak thrombin comparable to 300 nM emicizumab, while only ~3 nM was required to achieve comparable endogenous thrombin potential (ETP).

Collectively, these findings establish OctaV as a membrane-targeted dual cofactor with therapeutic potential for FVIII deficiency and combined FV/FVIII deficiency. Beyond its therapeutic potential, OctaV provides a unique platform to directly interrogate the spatial coupling of two key coagulation enzyme complexes that sequentially drive thrombin generation.

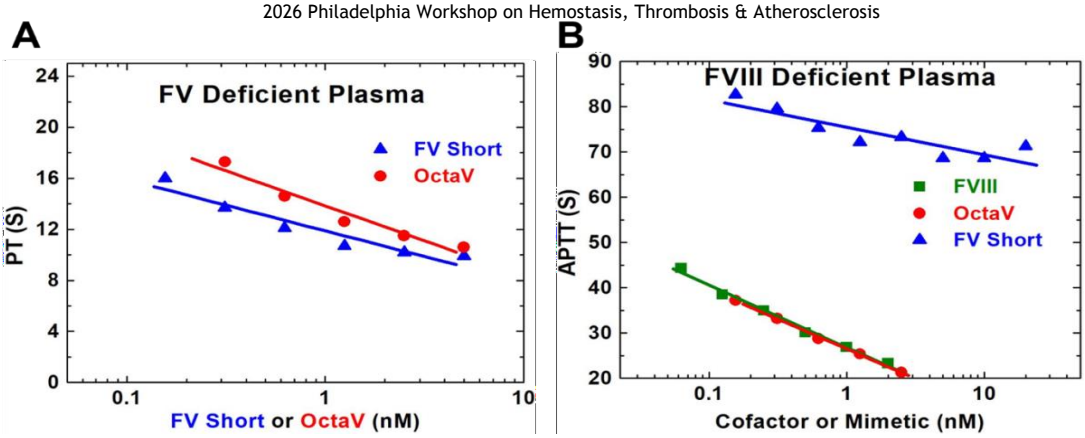


Figure: FV cofactor activity (A) and FVIII-mimetic activity (B) of OctaV assessed by PT and APTT respectively.

ABSTRACT 33:

A liver sinusoidal endothelial cell (LSEC)-directed genome editing platform for targeted integration at the F8 locus for hemophilia.

Jonathan Lindgren[1], Giulia Pavani[1, 2], Tyler Papp[3], Hamideh Parhiz[3], Denise Sabatino[1, 4]

[1]The Children's Hospital of Philadelphia, Center for Cellular and Molecular Therapeutics, Philadelphia, PA, United States, [2]Perelman School of Medicine, University of Pennsylvania, Department of Pathology and Laboratory Medicine, Philadelphia, PA, United States, [3]Perelman School of Medicine, University of Pennsylvania, Department of Systems Pharmacology and Translational Therapeutics, Philadelphia, PA, United States, [4]Perelman School of Medicine, University of Pennsylvania, Division of Hematology, Department of Pediatrics, Philadelphia, PA, United States

Hemophilia A (HA) is an X-linked bleeding disorder due to a deficiency in coagulation factor VIII (FVIII). Current adeno-associated virus (AAV)-based gene therapy approaches target FVIII expression to hepatocytes; however, the liver sinusoidal endothelial cells (LSEC) are the primary endogenous source of FVIII synthesis. We hypothesized that targeted gene editing of LSECs at the endogenous F8 locus could provide homeostatic and durable FVIII expression, overcoming key barriers of current gene therapies. To achieve LSEC-targeted editing, we developed a dual-delivery platform consisting of antibody-conjugated LSEC-targeted lipid nanoparticles (LNPs) to deliver the CRISPR-Cas9 mRNA and guide RNAs (sgRNAs), together with a bioengineered LSEC-tropic AAV capsid for donor template delivery. LNPs were conjugated to LSEC-specific monoclonal antibodies (LYVE-1 or CD31) via maleimide-thiol chemistry. Our genome editing strategy uses promoter hijacking by targeting insertion of the human F8 cDNA into the 5′ untranslated region (UTR) or exon 1 of the endogenous F8 locus, allowing expression to be driven by the native F8 promoter. To evaluate LNP tropism, LYVE1-LNPs, CD31-LNPs, or unmodified LNPs containing ZsGreen mRNA were administered intravenously to hem A/CD4KO mice. Twenty-four hours later, hepatocyte and non-parenchymal liver cell fractions were isolated and analyzed by flow cytometry.

LYVE1-LNPs demonstrated selective LSEC targeting, with 77% of LSECs (CD45−/CD31+/CD146+) expressing ZsGreen and minimal hepatocyte transduction (2%). CD31-LNPs achieved higher LSEC transduction (99%) but showed greater hepatocyte targeting (25%). To evaluate AAV and LNP co-targeting efficiency, mice received an engineered LSEC-targeted AAV (AAV-LSEC1) encoding eGFP (4 × 10^12 vg/kg), followed three weeks later by LNPs containing mCherry mRNA. Co-targeting was quantified as the percentage of GFP+mCherry+ LSECs. The highest co-targeting efficiency was achieved with LYVE1-LNPs (5mg), resulting in 23% dual-positive LSECs and minimal hepatocyte co-transduction (8%). These findings demonstrate the feasibility of simultaneous LSEC targeting using both AAV and LNP delivery platforms.

Additional dosing regimens may further refine the ability to co-target a larger portion of LSECs. For F8 editing by promoter hijacking, sgRNAs targeting the 5′UTR and early exon 1 of the murine F8 locus were screened in vitro. Guide performance ranged from 6.0% to 64.3% on-target editing efficiency, with the top-performing guides generating 34.5%, 38.0%, 53.3%, and 64.3% editing. The two most efficient guides (guide 6 and 7) were subsequently evaluated in vivo in wild-type mice using LYVE1-LNPs, CD31-LNPs, or unmodified LNPs carrying Cas9 mRNA and sgRNA. Functional disruption of endogenous F8 expression was assessed by FVIII activity (aPTT), while genome editing was quantified by Sanger sequencing of the F8 locus in isolated LSECs and hepatocytes as well as whole tissues (spleen, muscle (diaphragm), and lung). One month after LNP treatment, reductions in FVIII activity correlated with LSEC editing efficiency. CD31-LNP delivery of guides 6 and 7 produced the greatest reductions in FVIII activity (81.9% and 84.4% reduction in FVIII activity, respectively) and high genomic knockout scores in LSECs (79.0 and 68.0). LYVE1-LNP delivery of guides 6 and 7 resulted in 43.8% and 45.4% reduction in FVIII activity, with corresponding LSEC knockout scores of 34.7 and 32.7. Notably, LYVE1-LNPs showed no detectable editing in hepatocytes or extrahepatic tissues, whereas CD31-LNPs demonstrated low-level editing in the lung. Further studies to use these tools to deliver a donor template for targeted integration at the F8 locus are currently underway. Collectively, these studies establish novel LSEC-targeted LNP and AAV delivery systems capable of efficient and selective genome editing to the endogenous site of FVIII synthesis. This platform provides critical tools for targeted insertion of therapeutic F8 donor templates and may enable a durable, homeostatic, and mutation-agnostic gene-editing strategy for the treatment of hemophilia A.

ABSTRACT 34:

Hemostatic and Inflammatory Changes After SCI: Determining Temporal Coagulation and Neutrophil Dynamics

Olivia Parker*[1], Tanner Clifford*[1], Rebecca A. Risman, Ph.D.[1], Zachary Finkel, Ph.D.[1], Lauren Poole, Ph.D.[2], Rachel Weirnick[1], Chidera Ntiwunka-Ifeanyi[1], Mridul Dalmia[1], Azarin Reid[1], Ishaan Patil[1], Hajer Ali Sinan[1], Andrew R. Gosselin, Ph.D.[1], Julie Goswami, M.D.[3], Joseph Hanna, M.D.[4], Li Cai, Ph.D.[1], Valerie Tutwiler, Ph.D.[1]

*[1]Department of Biomedical Engineering, Rutgers University, Piscataway, New Jersey; [2] Department of Pharmacology, Rutgers Robert Wood Johnson Medical School, Piscataway, New Jersey, United States of America; [3]Department of Surgery, Rutgers Acute Care Surgery Research Laboratory (RASR), New Brunswick, New Jersey; [4]Department of Surgery, Division of Acute Care Surgery, Rutgers Robert Wood Johnson Medical School, New Brunswick, New Jersey (*Indicates co-first authorship)*

Spinal cord injury (SCI) poses an elevated risk for deep vein thrombosis within two weeks post-injury. However, little is known about the temporal changes in coagulation, fibrinolysis, and inflammation following SCI that may contribute to this thrombotic risk. Using human SCI patient data at hospital admission and an SCI mouse model, we investigated the interplay between SCI and hemostasis/inflammation from 1 to 14 days following SCI.

Following IRB approval, we assessed 63 trauma patients' blood plasma to delineate changes in coagulation and inflammatory profiles following injury. We compared human plasma proteomics coupled with coagulation kinetics using turbidity and clinical parameters (injury severity, activated Partial Thromboplastin Time) between SCI (n=6) and non-SCI patients (n=31). We also measured D-dimer concentration using ELISAs to assess fibrinolytic function post-injury.

Following IACUC approval, we used a T9-10 laminectomy model in mice (n=3) with a 50-70 kdyn contusion impact, to determine changes in coagulation and inflammation at 1, 3, 7, and 14 days post-injury (dpi). After animal sacrifice, the injured spinal cord tissue (lesion site) and blood were extracted to assess differences between sham (laminectomy) and injured mice (SCI). We measured platelet-poor plasma clotting kinetics using turbidity at 405 nm wavelength over 3 hours at 15-second intervals. Neutrophil Extracellular Traps (NETs), neutrophil-platelet aggregates, and leukocyte viability in the lesion site were quantified using immunohistochemistry (IHC). Genomic changes were quantified in both the blood and spinal cord-injured tissue (lesion site) using bulk RNA-seq. Ingenuity Pathway Analysis (IPA) was used to determine the pathways activated or inhibited across 1 to 14 dpi from bulk RNA-seq for both the blood and lesion site.

When comparing results from human patients who had experienced spinal cord injury (SCI) and non-spinal cord injury (Non-SCI) related traumas, blood was drawn from patients at similar times following injury (41 minutes vs. 43 minutes), and we observed that spine injury severity was positively correlated with neutrophil markers, while negatively correlated with fibrinolysis markers from proteomics analysis ($p<0.05$). Furthermore, we observed that SCI patients had less spontaneous lysis, higher D-dimer levels, and increased Activated Partial Thromboplastin Time compared to Non-SCI patients ($p<0.05$). Proteomic markers, Alpha-1-antitrypsin was increased, and Carboxypeptidase 2 was decreased in SCI patients compared to Non-SCI trauma patients ($p<0.05$).

In the days following injury in mice, there was a spike in activation in multiple thromboinflammatory pathways from IPA. NET Signaling and Cell Surface Interactions at the Vascular Wall, and Formation of Fibrin Clot (Clotting Cascade) were increased at 14 dpi, compared to previous time points in the blood. This spike was associated with a shorter clotting time in injured mice at 14 dpi compared to 1 dpi in turbidity clotting assays. IHC staining and imaging identified that leukocyte cell death was active at 3 dpi, along with platelet-neutrophil aggregates peaking at 3 dpi, along with NETs at 1 and 3 dpi in the lesion site. This was associated with pathways detected in IPA, such as Neutrophil Degranulation detected in the blood at 3 dpi. SCI has an altered fibrinolytic profile immediately after injury in human patients, while increased severity of injury is associated with neutrophil activity. This altered fibrinolytic profile and association with neutrophil activity observed in human patients may contribute to the hypercoagulable and neutrophil-related profile observed in mice, in the days to weeks following injury. In mice, leukocyte cell death is delayed until 3 dpi at the lesion site, corresponding to a thromboinflammatory state 72 hours post-injury. Then, two weeks post-injury, a hypercoagulable and thromboinflammatory state, evidenced by faster clot kinetics and activated neutrophil-and platelet-related pathways in the blood in mice, corresponds to the timing of heightened clotting risk observed clinically. These temporal dynamics in hemostasis and inflammation provide a

timeline for when therapeutics should be applied to abrogate inflammation and thrombosis. Future studies are needed to specifically determine the mechanistic link between inflammation and aberrant clotting after SCI.

ABSTRACT 35:

Inflammatory Pathways Regulate Cytokine Responses and Thrombotic Burden in Heparin-Induced Thrombocytopenia

Sophia Lazar[1], Trenton Hiatt[1], Steven E. McKenzie[1], & James V. Michael[1]

[1]The Cardeza Foundation for Hematologic Research, Center for Hemostasis, Thrombosis and Vascular Biology, Department of Medicine, Thomas Jefferson University, Philadelphia, PA

Background: Heparin-induced thrombocytopenia (HIT) is a severe prothrombotic immune complication driven by antibodies against platelet factor 4 (PF4)/heparin complexes.

Pathological immune complexes potently drive cellular activation of platelets and leukocytes, creating an imbalance between immune signaling and hemostasis. Despite major advances in diagnostics and anticoagulant management, clinical outcomes remain poor. Recent studies have identified multiple immune signaling checkpoints related to HIT-mediated pathological signaling, including the platelet-specific 12-lipoxygenase (ALOX12), and the NOD-like receptor protein 3 (NLRP3). Despite the central roles of platelets and immune signaling in HIT, the mechanisms connecting these responses remain incompletely understood.

Aims: This study aimed to investigate the contributions of NLRP3 and ALOX12 to HIT-mediated inflammation, and the subsequent effect on thrombosis *in vivo*. The secondary aim was to determine the influence of NLRP3 and ALOX12 on one another.

Methods: HIT IC challenge was performed in HIT mice expressing human FcγRIIA and human PF4 (hPF4) with or without genetic deletions of Nlrp3 or Alox12 through administration of heparin and the monoclonal anti-PF4/heparin antibody KKO. HIT WT, HIT × Nlrp3 KO, and HIT × Alox12 KO mice were additionally challenged with lipopolysaccharide (LPS) to compare responses to a distinct systemic inflammatory stimulus. Outcomes measured included platelet count, multiplex inflammation cytokine profiles, TAT complexes, 12-HETE, and survival.

Results: HIT IC challenge in HIT WT mice induced thrombocytopenia, a broad inflammatory cytokine response, and significantly elevated TAT levels. The combined inflammatory cytokine elevation correlated with TAT levels across HIT mice, supporting an association between systemic inflammation and thrombosis. Following HIT IC challenge, genetic deletion of either NLRP3 or ALOX12 did not have any role in promoting platelet clearance, though both knockout models exhibited reduced TAT levels and an overall reduction in the inflammatory cytokine response compared with HIT WT animals. While both knockout strains experienced thrombocytopenia, they had diminished thrombosis and cytokines; notably HIT x Alox12 KO mice had no detectable IL-1β . HIT IC challenge promoted a significant elevation to 12-HETE levels in HIT WT and HIT x Nlrp3 KO mice but was undetected in ALOX12 KO mice. LPS challenge elicited a greater overall inflammatory cytokine response, with distinct temporal kinetics compared with HIT IC challenge, distinguishing pathway-specific effects during HIT from responses to broader systemic inflammation. Following LPS challenge, ALOX12 deletion did not improve survival, whereas NLRP3 deletion was associated with improved survival at later time points.

Conclusion: HIT induces a broad inflammatory cytokine response that correlates with thrombotic burden. Reductions in TAT and inflammatory cytokine responses following NLRP3 or ALOX12 deletion implicate both pathways in the inflammatory and procoagulant response to HIT ICs. Preserved 12-HETE production following NLRP3 deletion, together with the overlapping effects of NLRP3 and ALOX12 deletion on HIT-induced inflammation, suggest that ALOX12 signaling may act upstream of NLRP3. The unique inflammation and survival profiles following HIT IC or LPS challenge further suggest differential reliance on platelet–immune signaling. Together, these findings strengthen the mechanistic link between platelet and innate immune cell signaling to promote inflammation, which correlates with thrombotic burden in HIT.

ABSTRACT 36:

Procoagulant activity reversion by hyperactive amino acid substitutions in hemophilia B-causing factor IX variants

Maxwell Chappell, Rose Kim, Kyumin Lee, Julia Q. Chau, and Benjamin J. Samelson-Jones

Division of Hematology, Department of Pediatrics, Children's Hospital of Philadelphia, Philadelphia, PA, 19104

Background: Hemophilia B (HB) is an inherited bleeding disorder due insufficient activity of clotting factor IX (FIX). The severity of the hemophilic phenotype varies from mild (5-40% FIX activity), to moderate (1-5% FIX activity), to severe (<1% FIX activity). HB is typically treated with FIX protein administration; recently, several adeno-associated viral (AAV) vectors capable of introducing a functional copy of the F9 gene and achieving mild-to-normal FIX levels have received regulatory approval. Alternative gene therapy approaches are needed since these AAV-based gene transfer products result in highly variable FIX activity levels and are not approved for pediatric patients.

Lipid nanoparticle (LNP)-delivered base editors may offer a solution to these problems. Approximately 70% of HB cases are the result of missense mutations. Direct application of base editing would only be able to correct a small fraction of these based on currently available edits with each disease-causing variant requiring a unique treatment. However, there are known gain-of-function (GoF) F9 variants (including R338L and R338Q) that exhibit FIX activities 4-10x higher than wild-type (WT) FIX. We hypothesize that the introduction of single nucleotide mutations leading to GoF effects can potentially compensate for the loss-of-function (LoF) HB-causing FIX missense substitutions. Notably, conversion from FIX WT to FIX R338Q is accessible with current cytosine base edits. Furthermore, the ability of GoF mutations to rescue HB-causing LoF mutations may inform on the structure-functional relationships of FIX.

Methods: LoF FIX plasmids were modified via mutagenesis to introduce the R338Q or R338L substitution and transfected into HEK 293 cells. Media was collected after 24 hours and tested for clotting activity using an activated partial thromboplastin time (aPTT) assay and antigen level using a FIX specific ELISA.

Results: To date, 33 HB-causing LoF FIX variants with a range of in vitro baseline activity have been screened in combination with R338Q. 16/21 (76.2%) severe FIX variants demonstrated enhanced activity, with 3/21 (14.3%) improving to a moderate or mild level. 4/4 (100%) moderate FIX variants demonstrated enhanced activity with 3/4 (75%) improving to a mild level. 2/3 (66.7%) mild FIX variants demonstrated enhanced activity, with both variants improving to a normal level. The remaining 5 variants had >40% FIX activity following transient transfection; 3/5 (60%) improved with R338Q insertion. Overall 25/33 (75.8%) HB-causing variants showed improvement in FIX procoagulant activity when combined with R338Q. 17 HB-causing FIX variants have been screened in combination with R338L. 9/10 (90%) severe FIX variants demonstrated enhanced activity with 3/10 (30%) improving to a moderate or mild level. 3/3 (100%) moderate FIX variants demonstrated enhanced activity with 2/3 (66.6%) improving to a mild level. 4/4 (100%) mild variants demonstrated enhanced activity with 2/4 (50%) improving to normal levels. Furthermore, 16/17 (94.1%) HB-causing variants showed improvement when combined with R338L. Of the variants screened with both R338Q and R338L, 12/13 (92.3%) showed improvement with both GoF variants.

Conclusions: Preliminary results suggest that combining hyperactive substitutions improves the procoagulant activity for the majority of HB-causing missense FIX variants. Interestingly, this enhancement with R338Q or R338L insertion is correlated with the enhancement we previously observed with emicizumab (Lee et al. *Blood*2024). These results support ongoing evaluation for developing base editing approaches to install GoF amino acid substitutions to revert procoagulant activity of HB-causing variants.

ABSTRACT 37:

Actomyosin-Dependent Platelet Remodeling in a Localized-Injury Model of Thrombus Formation Under Microvascular Flow

Taisia O. Shepeliuk[1], Rustem I. Litvinov[2], John W. Weisel[2], Fazly I. Ataullakhanov[1], Ekaterina L. Grishchuk[1]

[1]Department of Physiology, Perelman School of Medicine, University of Pennsylvania, Philadelphia, PA, USA; [2]Department of Cell and Developmental Biology, Perelman School of Medicine, University of Pennsylvania, Philadelphia, PA, USA

Platelet actomyosin-driven contractility generates forces that shrink and compact blood clots and thrombi. Much of our understanding of platelet-driven contraction comes from static clot-contraction assays, in which bulk clot shrinkage is observed after clot formation. Under flow, contractility has also been shown to compact and stabilize platelet aggregates; however, how actomyosin-dependent remodeling is integrated with continuous thrombus growth remains poorly understood. To address this question, we developed a custom-built microfluidic system for real-time imaging of the formation of a platelet-rich thrombus under arterial flow. Recalcified whole blood from healthy donors was perfused through a 100-μm-wide channel at a wall shear rate of 1,000 s^{-1} over a 50-μm-wide collagen/tissue factor activation strip, modeling a localized vascular injury. Platelets initially accumulated at the activation site, forming an anchored thrombus “head,” while subsequent growth extended downstream to form a thrombus “tail.” A fibrin-rich zone was located at the downstream edge of the head, beneath the floating tail. Scanning electron microscopy revealed marked regional differences in platelet morphology, ranging from loosely organized platelets with prominent filopodia to densely packed and flattened platelets, consistent with compaction. Real-time imaging did not reveal a late-onset bulk contraction; instead, internal remodeling continued throughout thrombus growth. Platelets incorporated at the downstream edge underwent collective retrograde displacement toward the anchored head, against the direction of flow. These movements began during the early stages of platelet accumulation, persisted throughout thrombus growth, and were detected at multiple depths within the growing thrombus. The rate of retrograde platelet movement was substantially reduced by blebbistatin, an inhibitor of non-muscle myosin II, demonstrating a strong actomyosin-dependent component. As expected, the total distance traveled by platelets toward the anchored head was also reduced, indicating decreased compaction of the developing thrombus. Surprisingly, blebbistatin also had a pronounced effect on the kinetics of thrombus growth. Growth initiated without an apparent lag but progressed more slowly, with a particularly marked reduction in the downstream tail. This slower growth was not accompanied by obvious fragmentation or detachment of the thrombus. The early emergence of the growth defect, diminished retrograde compaction in the presence of blebbistatin, and the absence of a late compaction event during normal growth are all consistent with actomyosin activity operating throughout thrombus formation rather than as a distinct late event. Together, these findings suggest that during active thrombus growth under flow, actomyosin activity supports both ongoing thrombus remodeling and the normal kinetics of thrombus formation.

ABSTRACT 38:
An Immuno-Coagulopathic Signature Predicts ADAMTS13 Activity on a Continuum in Pediatric TAMOF

Steven D. Ham, Nathan M. Diogo, Teresa Arroyo, Sydney A. Sheetz, Apoorva Babu, Stephen T. Famularo III, Samir U. Sayed, Richard Tustin III, Julie C. Fitzgerald, Michele P. Lambert, and Robert B. Lindell

Background: Thrombocytopenia-associated multiple organ failure (TAMOF) is a MODS phenotype, and we previously identified a proteomic signature implicating neutrophil activation and complement signaling in its pathology. We constructed a parsimonious 12-protein immuno-coagulopathic signature spanning immune dysregulation (VSIG4, IL15, SIGLEC10), endotheliopathy (VWF, ANGPT1, ANGPT2), complement regulation (PRELP, CD55, CD59), and platelet consumption (CCL5, PDGFA, EGF) that distinguished TAMOF from multiple organ failure without thrombocytopenia (MOF). TAMOF has previously been characterized by acquired ADAMTS13 dysfunction, thus we hypothesized that our immuno-coagulopathic signature could predict ADAMTS13 activity.

Methods: This single-center, prospective study enrolled patients within 48 hours of MODS onset. Plasma protein measurements with Nomic nELISA (Nomic Bio, Canada) were used to calculate immuno-coagulopathic signature scores for patients with platelet counts <100,000/mm³ (TAMOF) and without thrombocytopenia (MOF). Residual plasma was used for ADAMTS13 functional activity assays. We evaluated the relationship between immuno-coagulopathic score and ADAMTS13 activity using linear regression with adjustment for platelet count and illness severity (PELOD-2). Additionally, we tested for nonlinearity in the relationship using a restricted cubic spline in the unadjusted and adjusted models. Analyses were performed in R.

Results: Of 117 patients, there were 44 (38%) TAMOF and 73 (62%) MOF patients. There was a significant inverse association between immuno-coagulopathic score and ADAMTS13 activity after adjustment for platelet count and illness severity ($\beta = -57.8$; 95% CI −70.8, −44.8; $p < 0.0001$). The relationship between immuno-coagulopathic score and ADAMTS13 activity remained linear, with no evidence of nonlinearity in the unadjusted ($p=0.68$) or adjusted ($p=0.21$) spline models.

Conclusion: There is a continuous relationship between our immuno-coagulopathic score and ADAMTS13 activity, suggesting that the thromboinflammatory processes underlying TAMOF exist along a continuum. Thus, ADAMTS13 dysfunction may be a reflection of underlying immune dysregulation in TAMOF rather than the driving mechanistic process.

ABSTRACT 39:
Roles of Fibrin Clot Structure, Platelets, and Fibrinolysis in Endothelial Repair

Douglas Argueta[1], and Oleg V. Kim[1,2]

[1]Department of Biomedical Engineering, Virginia Tech, Blacksburg, VA, USA; [2]Department of Cell and Developmental Biology, University of Pennsylvania School of Medicine, Philadelphia, PA, USA

Following vascular injury, the hemostatic clot provides a fibrin matrix that influences subsequent endothelial repair. However, how fibrin network structure, platelets, and fibrinolysis affect reendothelialization remains incompletely understood. Here, we combined an in vitro model of endothelial repair with live-cell confocal imaging to examine how fibrin network architecture, platelets, and fibrinolysis influence endothelial cell migration, morphology, and gap closure. A defined gap was created in a human umbilical vein endothelial cell (HUVEC) monolayer using two-chamber culture inserts. Human citrated platelet-poor plasma (PPP) or platelet-rich plasma (PRP) was recalcified to form clots over the monolayer. Fibrin architecture was varied using thrombin concentrations of 0.3 and 1 U/mL, and abciximab (10 μg/mL) was used to inhibit platelet-mediated clot contraction in PRP samples. Endothelial repair was quantified by measuring gap width, area, and percentage closure over time. Fibrin network density and porosity were assessed from confocal images using Fiji.

Dense PPP clots strongly inhibited gap closure by restricting endothelial cell migration. Clots formed at the lower thrombin concentration had larger pores and supported migration and gap closure. In separate experiments, PRP clots also supported endothelial repair, although closure rates in both conditions remained significantly lower than under clot-free conditions.

Inhibition of platelet-mediated clot contraction with abciximab had little effect on gap closure, suggesting that contraction was not the primary driver of the enhanced repair observed with PRP clots. Platelet-derived signals, potentially including growth factors, may contribute to this effect. Tissue plasminogen activator (tPA)-induced fibrinolysis improved gap closure relative to untreated PPP clot conditions. Quantitative image analysis revealed significant differences in endothelial cell morphology between clot-containing and clot-free conditions, consistent with altered cell spreading and migratory behavior. Together, these findings show that fibrin clot structure, platelets, and fibrinolysis modulate endothelial cell migration and gap closure, helping explain how clots influence endothelial repair following vascular injury.

ABSTRACT 40:

Lipidomic Profiling Reveals Divergent Membrane Properties and Signaling in Neonatal and Adult Platelets

Rolf Dale P Bates[1*], Kimberley Banfield[2*], Nicholas Giroux[2], Rong Qiu[3], Erin Soule-Albridge[2], Amalia El Nems[2], Jesselin Romero Escobar[2], Martha Sola-Visner[2], Patricia Davenport[2^], Christopher S Thom[3,4^]

[1]Cell and Molecular Biology Graduate Group, University of Pennsylvania, Philadelphia, PA, USA; [2] Division of Newborn Medicine, Boston Children's Hospital and Harvard Medical School, Boston, MA, USA; [3] Division of Neonatology, Children's Hospital of Philadelphia, Philadelphia, PA, USA; [4] Department of Pediatrics, University of Pennsylvania Perelman School of Medicine, Philadelphia, PA, USA

**,^These authors contributed equally to this work*

Background: Standard clinical procedure to reduce baseline bleeding risk in preterm neonates utilizes prophylactic platelet transfusions at higher platelet count thresholds than in children and adults. However, these liberal platelet transfusion practices using banked adult platelets paradoxically *increase* bleeding, neurocognitive impairment, respiratory complications, and death in preterm neonates. Adult platelets are hyper-reactive and contain inflammatory molecules not found in neonatal platelets, while neonatal platelets show enrichment in proteins involved in metabolic activities, including lipid metabolism (Thom & Davenport *et al*, *JTH* 2024). Modulating banked adult platelets to adopt a hyporeactive neonatal phenotype could improve platelet transfusion safety in vulnerable newborns.

Objective: To define differences in the neonatal vs adult platelet lipidomes that explain developmental variation in platelet reactivity and inform safer platelet product design.

Methods: We collected 11 cord blood samples from full-term cesarean sections and 13 adult peripheral blood samples from healthy volunteers. Mass spectrometry was performed on isolated resting platelets for lipidomic and oxylipin analyses. Datasets were normalized to internal chemical standards and per-sample platelet count prior to statistical analysis.

Results: Platelets were isolated with mean CD41+ purity of 97.3% (cord blood) and 99.3% (adult). Resting platelets showed comparably low activation CD62P (MFI 432 cord blood, 315 adult). Of 1029 unique lipid species detected, we identified 591 significantly differentially abundant (BH-adjusted $p<0.05$) species. 235 species were enriched in neonatal platelets and 356 enriched in adult platelets. Neonatal and adult platelet samples clustered separately using principal component analysis (PC1, 58.4% of variance). We observed differential abundance of lipid species across all major lipid categories and classes, including phosphatidylethanolamines (PE), phosphatidylserines (PS), sphingomyelins (SM), ceramides (Cer), triacylglycerols (TG) and diacylglycerols (DG). Lipid set enrichment analysis (LSEA) identified coordinated shifts towards PS for neonates and TG and acylcarnitines for adults.

Adult platelets were enriched in pro-thrombotic and pro-inflammatory signaling intermediates, with higher abundance of oxylipin species derived from alpha-linolenic acid (ALA) and linoleic acid (LA) (24.2-fold, $p<1.2x10^{-5}$ and 9.0-fold, $p<4.1x10^{-6}$ respectively), as well as diacylglycerols (1.29-fold class-wide, $p<0.006$; top species up to 15.1-fold, $p<2.8x10^{-9}$). These shifts provide a basis for primed PKC recruitment and heightened downstream activation cascade activity.

To predict membrane biophysical properties, compositional proxies were used for membrane fluidity, including average acyl chain length, average unsaturation, polyunsaturated fatty acid (PUFA) percentage, and ceramide:sphingomyelin (Cer:SM) abundance ratio. Within plasma membrane-enriched lipid classes, adult platelets had modestly longer average acyl chain length (+0.17 carbons mean diff, $p<0.003$) and unsaturation adult platelets (+1.66%, $p<0.01$). Whole-lipidome Cer:SM ratio was higher instead in neonatal platelet lipidomes (1.63-fold, $p<9.0x10^{-4}$). Increased Cer:SM ratio impairs membrane fluidity, with increased Cer associated with membrane PS exposure, whereas higher SM proportion in adults may favor dynamic raft organization and receptor clustering. Opposing shifts in these metrics may reflect compensatory adjustments to preserve membrane function across developmental stage.

Conclusions: Neonatal and adult platelets have markedly distinct lipidomes. We reveal changes in lipids associated with membrane fluidity and secondary messenger signaling, potentially contributing to known differences in platelet reactivity. These findings provide an additional pathway to design platelet products with biological activity optimized for neonatal physiology.

The Children's Hospital of Philadelphia *presents*

The 54th Annual Philadelphia Workshop on Hemostasis, Thrombosis, & Atherosclerosis

A full day of scientific exchange in hematology – insights into basic, clinical, and translational research in coagulation, platelet biology, and blood therapies

We would like to sincerely thank our SPONSORS for their generous support:

ISTH 2021 VIRTUAL CONGRESS

MDPI

The Children's Hospital of Philadelphia®

Penn University of Pennsylvania Blood Centre

CELL Microsystems®

CHRONO-LOG CORPORATION

THE 54TH ANNUAL PHILADELPHIA WORKSHOP ON HEMOSTASIS, THROMBOSIS, & ATHEROSCLEROSIS

November 5, 2026 . 9 AM – 6 PM . William and Lois Kelley Research Building (KRB)